

# Polarimetric variations of binary stars. V. Pre-main-sequence spectroscopic binaries located in Ophiuchus and Scorpius<sup>1</sup>

N. Manset<sup>2</sup> and P. Bastien

*Département de Physique, Université de Montréal, C.P. 6128, Succursale Centre-Ville, Montréal, QC, H3C 3J7, Canada, and Observatoire du Mont Mégantic*

manset@cfht.hawaii.edu, bastien@astro.umontreal.ca

## ABSTRACT

We present polarimetric observations of 7 pre-main-sequence (PMS) spectroscopic binaries located in the  $\rho$  Ophiuchus and Upper Scorpius star forming regions (SFRs). The average observed polarizations at 7660Å are between 0.5% and 3.5%. After estimates of the interstellar polarization are removed, all binaries have an *intrinsic* polarization above 0.4%, even though most of them do not present other evidences for circumstellar dust. Two binaries, NTTS 162814-2427 and NTTS 162819-2423S, present high levels of intrinsic polarization between 1.5% and 2.1%, in agreement with the fact that other observations (photometry, spectroscopy) indicate the presence of circumstellar dust. Tests reveal that all 7 PMS binaries have a statistically variable or possibly variable polarization. Combining these results with our previous sample of binaries located in the Taurus, Auriga and Orion SFRs, 68% of the binaries have an intrinsic polarization above 0.5%, and 90% of the binaries are polarimetrically variable or possibly variable. NTTS 160814-1857, NTTS 162814-2427, and NTTS 162819-2423S are clearly polarimetrically variable. The first two also exhibit phase-locked variations over  $\sim 10$  and  $\sim 40$  orbits respectively. Statistically, NTTS 160905-1859 is possibly variable, but it shows periodic variations not detected by the statistical tests; those variations are not phased-locked and only present for short intervals of time. The amplitudes of the variations reach a few tenths of a percent, greater than for the previously studied PMS binaries located in the Taurus, Orion, and Auriga SFRs. The high-eccentricity system NTTS 162814-2427 shows single-periodic variations, in agreement with our previous numerical simulations. We compare the observations with some of our numerical simulations, and also show that an analysis of the periodic polarimetric variations with the Brown, McLean, & Emslie (1978) formalism to find the orbital inclination is for the moment premature: non-periodic events introduce stochastic noise that partially masks

---

<sup>1</sup>Based in part on observations collected with the 2m Bernard-Lyot telescope (TBL) operated by INSU/CNRS and Pic-du-Midi Observatory (CNRS USR 5026). Financial support for the observations at Pic-du-Midi was provided by the *Programme National de Physique Stellaire* (PNPS) of CNRS/INSU, France.

<sup>2</sup>Now at: Canada-France-Hawaii Telescope Corporation, 65-1238 Mamalahoa Hwy, Kamuela, HI 96743, USA

the periodic variations and prevents the BME formalism from finding a reasonable estimate of the inclination.

*Subject headings:* binaries: close — circumstellar matter — methods: observational — stars: pre-main-sequence — techniques: polarimetric

## 1. Introduction

Pre-main-sequence (PMS) stars are objects still contracting to the main sequence and surrounded by disks and/or envelopes of circumstellar dust and gas. The dust grains produce polarization by scattering (see Bastien 1996 for a review). In PMS binary systems, the circumstellar matter may be found around each star (circumstellar disk, or CS disk) and/or around the binary itself (circumbinary disk, or CB disk).

We have shown (Manset & Bastien 2000, 2001a, hereafter Papers I and II) how the linear polarization of a binary surrounded by circumstellar matter varies periodically as a function of the orbital period, and how the geometry of the disks, the nature and characteristics of the scatterers, the masses of the stars, and the orbit characteristics affect the polarimetric curves. Models can be used to find the orbital inclination from those polarimetric variations (see for example Rudy & Kemp 1978; Brown, McLean, & Emslie 1978). The work from Brown et al. (hereafter BME) uses first- and second-order Fourier analysis of the Stokes curves to give, in addition to the orbital inclination, moments related to the distribution of the scatterers in the CS and CB environments. The BME formalism was developed for Thomson scattering in optically thin envelopes, and for binaries in circular orbits. Since polarization in PMS stars is produced by scattering on dust grains, and most of the known spectroscopic PMS binaries have eccentric orbits, the BME formalism cannot be used a priori. However, we have shown (Papers I and II) that the BME analysis can still be applied in those cases, with a few limitations.

In this context, we have obtained polarimetric observations of 24 spectroscopic PMS binaries. Detailed analyses were presented for the only Herbig Ae/Be binary of our sample, MWC 1080 (Manset & Bastien 2001b, hereafter Paper III), and for 14 PMS binaries located in the Taurus, Orion, and Auriga SFRs (Manset & Bastien 2002, hereafter Paper IV). MWC 1080's polarization and position angle are clearly variable, at all wavelengths, and on time scales of hours, days, months, and years. Stochastic variability is accompanied by periodic variations caused by the orbital motion of the stars in their dusty environment. The variations are not simply double-periodic (seen twice per orbit) but include single-periodic (seen once per orbit) and higher-order variations.

The analysis of 14 PMS binaries located in the Taurus, Auriga, and Orion SFRs revealed that after removal of estimates of the interstellar polarization, about half the binaries have an *intrinsic* polarization above 0.5%, even though most of them do not present other evidences for the presence of circumstellar dust. Various tests reveal that 77% of those PMS binaries have or possibly have

a variable polarization. The polarimetric variations are noisier and of a lesser amplitude ( $\sim 0.1\%$ ) than for other types of binaries, such as hot stars. We have shown that an analysis of the periodic polarimetric variations with the BME formalism to find the orbital inclination is for the moment premature: non-periodic events introduce stochastic noise that partially masks the periodic low-amplitude variations and prevents the BME formalism from finding a reasonable estimate of the orbital inclination.

Here we report the complete observations and detailed analysis for the PMS binaries located in the  $\rho$  Ophiuchus and Upper Scorpius SFRs.

## 2. Observations

The stars were chosen mainly from the list of binaries found in Mathieu (1994), to which we added subsequent discoveries. Tables 1 and 2 present basic information (other names, coordinates, location), and spectroscopic and orbital data (spectral type, PMS type, orbital period and eccentricity, orbital inclination when known, and distance) for 7 of the binaries located in the  $\rho$  Ophiuchus and Upper Scorpius SFRs.

The binaries were observed at the Observatoire du Mont Mégantic (OMM), Québec, Canada, between 1995 May and 1999 June, using a  $8''.2$  aperture hole and a broad red filter (RG645: 7660 Å central wavelength, 2410 Å full width at half maximum). Polarimetric data were taken with Beauty and The Beast, a two-channel photo-electric polarimeter, which uses a Wollaston prism, a Pockels cell, and an additional quarter-wave plate. The data were calibrated for instrumental efficiency, instrumental polarization (due to the telescope’s mirrors), and zero point of position angle, using a Glan-Thomson prism, non-polarized standard stars, and polarized standard stars, respectively. On average, the instrumental polarization was very low ( $0.020\% \pm 0.015\%$ , never above 0.03%) and negligible, which simplifies the determination of both instrumental polarization and origin of position angle. The observational errors were calculated from photon statistics, and also include uncertainties introduced by the previously mentioned calibrations. The final uncertainty on individual measurements of the polarization  $P$  is usually in the range 0.03–0.05%. The relative errors in position angle  $\theta$  can be as low as  $0.1^\circ$ , but due to instrumental effects, systematic errors, and the calibration procedure itself, the absolute errors on the position angles are of the order of  $1^\circ$ . For more details on the instrument and the observational method, see Manset & Bastien (1995, 2001b) and Manset (2000). Table 3 summarizes the observations and gives the average polarization and position angle along with the number of observations.

Data were also obtained in 1994 with the polarimeter STERENN at the 2-meter Bernard-Lyot Telescope of the Observatoire du Pic-du-Midi (OPdM), France. This 2-channel polarimeter uses a half-wave plate rotating at 20 Hz and a Wollaston prism, along with S-20 photo-multiplier tubes sensitive to the  $UBV$  domain. A Johnson  $V$  filter was used, along with a  $10''$  aperture hole. Instrumental efficiency and instrumental polarization were measured with polarized and

non-polarized standard stars, respectively. The observational errors were calculated from the fit of the observations to a sinusoid function, and range between 0.05% and 0.10% on individual measurements.

### 3. Estimation of the interstellar polarization

Polarimetric observations are usually a sum of interstellar (and sometimes also intra-cluster) and intrinsic polarizations. An estimation of the interstellar (IS) polarization for each object observed can be used to assess the presence of intrinsic polarization. We have used the Heiles (2000) catalog of over 9000 polarization measurements to determine if the observed polarization for the PMS binaries studied here is of intrinsic or IS origin, or a combination of both. This catalog is an improvement over the one from Mathewson et al. (1978): it contains additional observations, all data have been verified, and more precise coordinates are given.

For each observed PMS binary, the catalog was scanned to select at least  $\approx 20$  stars *with a similar distance*. Depending on the stellar density and number of measurements in the catalog, this led to the selection of a region between  $6^\circ$  and  $10^\circ$  in radius around the target, and within 62 to 80 pc of it. The stars selected from the catalog are used to compute an average of the IS polarization in that region around the target, and also to find an average ratio of the polarization to color excess  $P/E(B - V)$ . The IS position angle is calculated with a simple average and with a distance-weighted average of the polarization of all the stars selected; this method also gives more weight to high IS polarization values (for which the position angle is well determined) than to low polarization values (which have poorly-determined position angles). In all the cases here, the two IS position angle values are similar within their uncertainties, which indicates that the alignment is generally good over all of the region studied, and that the IS polarization value estimated is reliable. However, if the IS position angles are not well aligned, the average IS polarization value  $P_{\text{IS}}$  will be too low (since the vectors cancel out). We therefore use a different method to find the IS polarization<sup>3</sup>. Based on an extinction value for the targets and assuming that this extinction is of IS origin only, an estimate of the IS polarization is found from the average ratio  $P/E(B - V)$ .

If the position angles for the IS polarization and for the target are different, it points to an intrinsic origin for at least part of the polarization measured. Intrinsic polarization is also deduced from polarimetric variability.

Results are presented in Table 3, where the weighted averages of the observed  $P$  and  $\theta$  for the binaries are given along with the possible origin of the observed polarization: a  $\star$  symbol indicates intrinsic polarization while IS stands for interstellar polarization<sup>4</sup>. When IS comes before

---

<sup>3</sup>This is the reason why the errors for  $P_{\text{IS}}$  and  $\theta_{\text{IS}}$  are not related by their usual relation,  $\sigma_\theta = 26.85\sigma_P/P$ .

<sup>4</sup>Table 3 includes the correct interstellar polarization and intrinsic polarization estimates for the binaries presented in Paper IV, in which the values of  $P_{\text{IS}}$  given were computed with an inappropriate method (vectorial average of the

a  $\star$  symbol, the IS component of the polarization is probably stronger than the intrinsic one, and vice versa. The following columns present our calculation of the IS polarization (polarization and position angle, along with their uncertainties), based on the method presented above. We also give  $N_{IS}$ , the number of measurements used to estimate this IS polarization, and the radius and the interval of distance of the region considered. Subtracting the IS polarization from the observed one gives the intrinsic polarization, shown in the last columns.

Note that the IS polarization given in columns 6–9 of Table 3 is only an *estimate* for the *whole region* around a binary, and in some cases might not apply to a given binary. In particular, it may include CS or intra-cluster material and then over-estimates the IS polarization. Consequently, the intrinsic polarizations given in the last columns should be considered crude estimations only, intended to give an idea of the polarimetric characteristics of the observed binaries as a whole, and not definitive values of the intrinsic polarization for each binary.

To determine if an observed polarization has an IS component, we give more weight to the value of  $\theta_{IS}$  deduced from neighboring stars than to  $P_{IS}$  which depends on the value  $E(B - V)$  given to a target. Since  $P_{IS}$  can include the effect of CS material and not just that of IS dust, it is less reliable. We do not have the wavelength dependence of the polarization, which can usually be used to extract the IS component. To help determine if there is an intrinsic component of polarization, we also use the level of polarimetric variability since IS polarization is stable.

#### 4. Polarimetric variability

Since a majority of single PMS stars are variable polarimetrically (Bastien 1982; Drissen, Bastien, & St-Louis 1989; Ménard & Bastien 1992), we also expected PMS binaries to be polarimetrically variable, either periodically or not. We have found that 77% of our 14 PMS binaries located in the Taurus, Auriga, and Orion SFRs are variable or suspected variable. Various tests were applied to check the polarimetric variability or stability of PMS binaries: minimum and maximum values, variance test,  $Z$  test, and finally, a  $\chi^2$  test.

One crude but easy way to check for variability in a set of observations is to compare the difference between the maximum and minimum values of a quantity with its average or typical observational uncertainty; variable observations will have maximum and minimum values well outside the range expected from the observational uncertainty. One can calculate the variance of the sample (which is a measure of the “width” of the observations, or of the scatter from the mean, or of the “variability” around a central value), and compare it to the standard deviation of the mean, which gives the error from photon statistics as if all the observations had been added together. For a set of observations of a non-variable quantity, the sample variance will be low (the observations are all clustered closely to the mean) and similar to the standard deviation of the mean. But if

---

polarization). Thus, Paper IV under-estimated the IS polarization.

there is variability, the “width” of the observations will be greater than the standard deviation of the mean.

For the  $Z$  test, if the data are “well behaved” or “consistent”,  $Z \approx 1$  within its standard error  $\sigma_Z$ . If  $Z$  differs from  $1 \pm \sigma_Z$ , then there may be variability. Lastly,  $\chi^2$  values are calculated for  $Q$  and  $U$  separately, using  $1\sigma_i$  and  $1.5\sigma_i$ . The probability of obtaining a given value of  $\chi^2$  in a Gaussian distribution is found for each of the four  $\chi^2$  values. We define the criteria as follows: the star is variable if at least 2 of the four  $\chi^2$  values are over 0.95; the star is suspected to be variable if one out of four  $\chi^2$  values is over 0.95. We developed in Paper IV a protocol on how to interpret the results of these tests in order to assign the polarization of a star as being variable, suspected variable, possibly constant, or constant. We refer the reader to Paper IV for more information.

Many PMS binaries in this sample and in the Taurus, Auriga, Orion sample (Paper IV) show observations with polarization levels and/or position angle well below or above the bulk of the data. We call these observations “atypical” but they are nonetheless real. Close examination of polarization observations taken over 5 years of non-polarized standard stars (84 observations), polarized standard stars (53 observations), 3 stars that were followed for many consecutive hours (121 observations) did not show atypical observations like the ones we repeatedly saw for PMS binaries (Manset 2000). Therefore, we believe these atypical observations were due to some eruption-like events or significant modifications in the CS environment (e.g., formation/destruction of condensations, accretion events), and not because of instrumental problems. Since this study of binary PMS stars is more concerned with orbit-induced, “typical”, polarimetric variations than with random, atypical ones, we have removed the atypical observations before using the variability tests. This allows us to study the more typical variations.

Table 4 presents the amplitude of the polarimetric variations for all binaries of our sample, including MWC 1080 (Paper III), the binaries located in the Taurus, Auriga, and Orion SFRs (Paper IV), and 2 systems which will be presented in future papers. The amplitudes were calculated by simply taking the difference between the minimum and maximum values of  $P$ ,  $\theta$ ,  $Q$  and  $U$ ; note that for some cases, atypical observations were not considered so that the more typical variations could be characterized. The variations (in  $Q$  or  $U$ ) generally have amplitudes up to 0.3%. Two binaries, NTTS 162814-2427 and NTTS 162819-2423S, present much higher variations, at the 1% level. This indicates that, first of all, there is enough dust in the environment of these 2 systems to produce the polarization, and second, that the configuration is favorable to high-amplitude variations. Since these variations are not clearly periodic, an alternative explanation would rely on these systems being very active (eruptive-like events, strong modifications of the CS environment) and not on orbit-induced variations. In our previous numerical simulations, the highest amplitude variations were produced with CS disks instead of CB disks, but we were not able to produce variations above a few tenths of a percent (Paper II).

The details of the variability tests are shown in Table 5, where we give for each star the number of observations used for the variability tests,  $\sigma_{\text{sample}}$  and  $\sigma_{\text{mean}}$ ,  $Z$  and its standard error, and  $P\chi^2$ ,

calculated with  $1\sigma$  and  $1.5\sigma$ . The conclusions of the variability tests are shown in Table 6, where we have classified the stars as “variable”, “suspected variable”, and “possibly constant”. Of the 7 binaries, 3 are statistically variable (NTTS 160814-1857, NTTS 162819-2423S, and NTTS 162814-2427) and the others are suspected to be variable (NTTS 155808-2219, NTTS 160905-1859, Haro 1-14C, NTTS 155913-2233). When combined with the results from Papers III and IV, 90% of the PMS binaries (19/21) are variables or suspected variables, in agreement with the results found by Bastien (1988) and Ménard & Bastien (1992) for a sample of mostly single PMS stars.

## 5. Periodic polarimetric variations

In addition to the general variability, which is a known property of single PMS stars, PMS binaries will also present periodic polarimetric variations caused by the orbital motion, even if in some cases the amplitude may be too small to be detected with the currently available instruments or masked by non-periodic or pseudo-periodic variations. In the case of Mie scattering, we have also shown in Paper II that dust grains, which are mostly responsible for the polarization, are less efficient polarizers and produce smaller amplitude variations than electrons. This is an indication that periodic polarimetric variations could be more difficult to observe in PMS binaries than in, for example, hot binaries surrounded by electrons, which can easily exhibit variations of a few tenths of a percent (see for example Robert et al. 1990; Robert et al. 1992). The size of the grains also determines the amplitude of the polarimetric variations: dust grains with radii  $\sim 0.1\mu\text{m}$  produce the largest polarimetric variations (Paper II).

To look for periodic polarimetric variations, the known orbital periods are used to calculate the orbital phase for each measurement. The polarization  $P$ , its position angle  $\theta$ , and the Stokes parameters  $Q$  and  $U$  are plotted as functions of the orbital phase (see Figures 1, 3 – 6, 8 – 13, 15 – 17). When enough data are available, observations are represented as first and second harmonics of  $\lambda = 2\pi\phi$ , where  $\phi$  is the orbital phase:

$$Q = q_0 + q_1 \cos \lambda + q_2 \sin \lambda + q_3 \cos 2\lambda + q_4 \sin 2\lambda, \quad (1)$$

$$U = u_0 + u_1 \cos \lambda + u_2 \sin \lambda + u_3 \cos 2\lambda + u_4 \sin 2\lambda. \quad (2)$$

The coefficients of this fit are then used to find the orbital inclination, following the BME formalism and using the first and second order Fourier coefficients:

$$\left[ \frac{1 - \cos i}{1 + \cos i} \right]^2 = \frac{(u_1 + q_2)^2 + (u_2 - q_1)^2}{(u_2 + q_1)^2 + (u_1 - q_2)^2}, \quad (3)$$

$$\left[ \frac{1 - \cos i}{1 + \cos i} \right]^4 = \frac{(u_3 + q_4)^2 + (u_4 - q_3)^2}{(u_4 + q_3)^2 + (u_3 - q_4)^2}. \quad (4)$$

The representation with sinusoids is a useful representation of orbit-induced variations, and is not used only to apply the BME formalism.

For 5 of the 7 binaries, we have enough data to look for periodic variations, and some of them do show periodic variations (see below). However the curves representing the fits made according to Eq. 1 and 2 do not always represent the observations well, for various reasons. Effects induced by dust instead of electrons as scatterers, elliptical instead of circular orbits, and variable absorption effects may produce variations which may not be well represented by the first and second harmonics only. The fitted curves are nevertheless a useful representation of the data and illustrate how the BME formalism, extended by the numerical simulations of Papers I and II, can be applied.

Periodic polarimetric variations can be caused by the binarity (orbital motion) or the presence of hot or cool stellar spots, among a few reasons. Classical T Tauri Stars (CTTS) are known to have both cool and hot spots, and WTTS generally have only cool spots (Bouvier et al. 1993), some of which can be stable over periods of several months (on V410 Tau for example, Herbst 1989). Since all the binaries observed here are WTTS and in general display only small photometric variations, we believe that the spots causing the photometric variations, if present, are small, and have a very small effect on the polarization. In addition to stellar spots, non-periodic phenomena such as eruptive events, variable accretion and rearrangements of the CS or CB material can cause pseudo-periodic polarimetric variations that may mask the strictly periodic ones, especially if the observations are taken over many orbital periods, as is the case here.

Despite these difficulties, some binaries present periodic variations: NTTS 160814-1857, NTTS 162814-2427, NTTS 160905-1859 (for short intervals of time), and NTTS 155913-2233 (low-amplitude variations seen when the data are binned). To investigate the significance of this periodicity, a Phase Dispersion Method (Stellingwerf 1978) and a Lomb normalized periodogram algorithm (Press et al. 1997) were used. The Phase Dispersion Method (PDM) is a least-squares fitting technique suited for non-sinusoidal time variations covered by irregularly spaced observations, and finds the period that produces the least scatter about the mean curve. The Lomb normalized periodogram (LNP) method is more powerful than Fast Fourier Transform methods for uneven sampling, but still assumes the curve is sinusoidal, which may not be always appropriate for the polarimetric observations presented here. The periods found by using both methods are very similar to one another for a given star, but the significance is usually marginal.

NTTS 162814-2427 presents single-periodic variations readily seen in position angle and  $U$  (see Figure 16). The PDM finds in the position angle data a period of  $35.4d$ , and the LNP has two peaks, at  $35.7$  and  $32.7d$ , but those 3 peaks are local extrema with other periods coming up with similar significance. Therefore, we cannot attribute a strong significance to those peaks. When using the binned data instead of the whole set of observations, the LNP recognizes the presence of periodicity and the period found has a 60% probability of not coming from random Gaussian noise, which is only slightly better than chance. Those periods compare rather well with the known orbital period of  $35.95d$ . NTTS 162814-2427 does show variations with amplitudes of a few tenths of a percent. Our numerical simulations can produce amplitudes of  $\sim 0.1\%$  if there is a CS disk but no CB disk. NTTS 162814-2427 shows strong single-periodic variations, which we attribute to the large orbital eccentricity. For most of the other binaries, the presence or absence of  $1\lambda$  variations,



and the exact cause of the single-periodic variations, if present, are harder to determine.

We will now discuss individual stars.

## 6. Comments on individual stars

The detailed observations are presented in Tables 7 to 15 and in Figures 1 to 17.

### 6.1. NTTS 155808-2219 = ScoPMS 20

This 16.95-day binary (Mathieu 1994) has a projected separation of 0.048 AU (Jensen, Mathieu, & Fuller 1996), and there is a tertiary component (Mathieu, Walter, & Myers 1989; Walter et al. 1994). The radial velocity measurements exclude membership in the Upper Scorpius association (Walter et al. 1994). The primary has a rotation period of 4.30 d (Adams, Walter, & Wolk 1998).

Data for NTTS 155808-2219 are presented in Table 7 and Figure 1. The statistical tests conclude that the average polarization at 7660Å, 0.48% at 139°, is possibly variable (see Tables 5 and 6). This conclusion is based on only four observations that show a constant polarization but one position angle well above the others. From the polarization catalog of Heiles (2000), we find an average IS polarization of  $0.34 \pm 0.07\%$  at 88° (see Table 3 and the map on Figure 2). This value was found by averaging the polarization of 22 neighboring stars located within 6° and 80 pc of NTTS 155808-2219. The binary presented in the next section, NTTS 155913-2233, is 0.35° from NTTS 155808-2219 and also has a very similar polarization, 0.49% at 124°, which points to a common IS polarization for both binaries. Since the observed and IS position angles are different and NTTS 155808-2219 is possibly variable, we conclude that its polarization is the sum of intrinsic and IS polarization.

### 6.2. NTTS 155913-2233 = ScoPMS 23

This 2.42378-day binary (Mathieu et al. 1989) is a double-lined system (Prato & Simon 1996) with a separation of 0.014 AU (Jensen et al. 1996). A weak tertiary component was detected spectroscopically (Mathieu et al. 1989) and found to be at large distance from the binary since its effect on the velocities of the binary or the tertiary itself was not detected. It was later detected in a 2.2 μm speckle imaging survey, at a separation of 0".288 (or 45 AU at a distance of 160 pc) and position angle 347° (Ghez, Neugebauer, & Matthews 1993). It is included in our 8".2 aperture hole. The two stars of the spectroscopic binary are K5 and M5 stars, the third star is a K5, and the mass ratio of the spectroscopic binary is  $2.1 \pm 0.24$  (Prato & Simon 1996). The primary has a rotation period of 3.30 d (Adams et al. 1998). There is no evidence for extended circumstellar material, either in low-dispersion spectroscopic or IR photometric data; there is no evidence for an

associated disk, mass accretion or mass loss (Mathieu et al. 1989). Although it is young, with an age of  $10^6$  yr (Mathieu et al. 1989), it is a mature system, with a circular orbit and no evidence for circumstellar material.

Data are presented in Tables 8 and 9, and in Figures 3, 4, and 5. The polarization is similar at  $7660\text{\AA}$  and  $5550\text{\AA}$ . Statistical tests do not indicate any variability at  $5550\text{\AA}$ , but this might be due to the small number of observations and the relatively high uncertainties. At  $7660\text{\AA}$ , the binary seems to be more variable than at  $5550\text{\AA}$ ; statistical tests indicate that NTTS 155913-2233 is possibly variable (Table 6). Figure 3 shows variations with an peak-to-peak amplitude of 0.2% in  $P$ , to be compared with the average uncertainty 0.042%. No periodic variations are seen. There might be two different epochs, one from 1995 May to 1996 May and having a peak in polarization at phases 0.3-0.4, and the second from 1997 April to 1997 June, with a peak at phases 0.5-0.6. However, the data from these two epochs do not show any more periodic variations than all of the data combined. Figure 4 presents the observations, where the period has been divided into 20 bins, and the data averaged in each bin. The binned data may show low-amplitude periodic variations. The orbit is almost circular, but variations are not purely double-periodic. Data obtained at  $5550\text{\AA}$ , presented in Figure 5, show a systematic (as opposed to random) variation of the position angle. These variations cover a different time interval and are not similar to those seen at  $7660\text{\AA}$ .

Two atypical observations are not shown in the figures for the  $7660\text{\AA}$  data and were not used in the variability calculations. These 2 measurements were taken almost 2 years apart, but have similar position angles,  $162^\circ$  and  $168^\circ$ , very different from the rest of the observations ( $124^\circ$ ). The first atypical observation has a polarization lower than the rest of the data, but the second has a polarization very similar to the general polarization observed. We believe these 2 atypical observations are evidence for significant transient changes in this system, an eruptive-like event at the surface of one of the stars or a change in the matter distribution, for example. Such atypical polarizations or positions angles have been observed before in the HAeBe binary MWC 1080 (Paper III) and other PMS binaries (Paper IV). These non-periodic variations are also in agreement with the general polarimetric variability observed in single PMS. Since NTTS 155913-2233 is  $0.35^\circ$  from NTTS 155808-2219 (see map in Figure 2), has a very similar polarization, and is possibly constant, we conclude that the observed polarization is the sum of intrinsic and IS polarization.

### 6.3. NTTS 160814-1857 = HBC 630 = ScoPMS 44

Although this 144.7-day binary (Mathieu 1994) is identified as 'tt' in the HBC catalog, Walter (1986) identifies it as a NTTS; its  $H\alpha$  line is in emission, with  $W_\lambda = 0.6 \text{\AA}$ . The projected separation of this single-lined spectroscopic binary is 0.19 AU (Jensen et al. 1996). It is not found in the IRAS Point Source Catalog but there is a flat NIR excess that can be modeled by adding to the K2 IV primary a cool M3 IV companion 3.7 mag fainter than the primary at  $V$ , although this is not a unique solution; the non spectroscopic detection of the secondary suggests that the luminosity ratio exceeds 10:1 (Walter et al. 1994). According to Zakirov et al. (1993), brightness variations in  $V$

had an amplitude of 0.16 mag in 1991/1992, with a rotational period of 3.81 d; no eclipsing effect could be found. Spectroscopic evidence argues against the presence of significant circumstellar material (Walter 1986).

Data are presented in Table 10 and Figure 6. The average polarization at 7660Å, 1.94% at 117°, is statistically variable (see Table 5 and 6); the single observation made at 5550Å is lower than the 7660Å values, by  $\sim 0.3\%$ , but the position angle is similar. Even though spectroscopic observations do not indicate the presence of CS material (Walter 1986), the intrinsic polarization is significant (0.7%) and variations are present. The nine observations taken at 7660Å, which were taken over  $\approx 8$  orbits, are very well fitted by the theoretical sinusoidal curves, and do not show the scatter usually observed. For example, GW Ori, for which we have 11 observations taken over  $\approx 4$  orbits, does not show variations as well behaved as those in NTTS 160814-1857 (Paper IV). Differences in the CS and CB environment (configuration or stability) are probably the explanation. The catalog from Heiles (2000) shows that the IS polarization is lower than the observed one,  $1.51 \pm 0.26\%$  at 123° (see map in Figure 7). The similar IS position angle indicates the presence of IS polarization. Since NTTS 160814-1857 is polarimetrically variable, we conclude that its polarization is the sum of strong IS and weaker intrinsic components.

#### 6.4. NTTS 160905-1859 = HBC 633 = ScoPMS 48

This 10.4-day binary (Mathieu 1994) is also identified as 'tt' in the HBC catalog but Walter (1986) identifies it as a NTTS; the H $\alpha$  line is seen in *absorption* with  $W_\lambda = 0.6 \text{ \AA}$ . The projected separation of this single-lined spectroscopic binary is 0.015 AU (Jensen et al. 1996). It is not found in the IRAS Point Source Catalog but the small excess in NIR (smaller than the one for NTTS 160814-1857), could be due to the companion, which would then be 4 mag fainter at V, although this is not a unique solution. Non-detection of the secondary in spectroscopic observations suggests that the luminosity ratio exceeds 10:1 (Walter et al. 1994). Spectroscopic evidence argues against the presence of significant circumstellar material (Walter 1986). The derived age,  $7 \times 10^6$  yr, makes it one of the oldest WTTS (Mathieu et al. 1989).

NTTS 160905-1859 is 0.2° from NTTS 160814-1857 (see map in Figure 7). It has a slightly lower polarization average of 1.38% at 134° (see Table 3). It is a suspected variable (see Table 6). As for the previous binary, we conclude that its polarization is the sum of IS and intrinsic components.

Data are presented in Tables 11 and 12, and in Figure 8 to 12. As was the case for NTTS 160814-2427, the polarization at 5550Å is lower than the observations taken at 7660Å by about  $\sim 0.3\%$ , but the position angles are all very similar. This binary shows some signs of variability at 7660Å but not at 5550Å. The first figure shows all the data taken at 7660Å except two atypical observations that stand out from the bulk of the data. These two measurements, taken 2 years apart, present position angles (141° and 121°) different than the average (134°) although the polarization levels are typical of this star. These atypical observations are the result of some non-periodic change in

the CS or CB environment. The figure also shows that there is a lot of scatter and no obvious periodic variations. If we divide the data in different epochs of observations, we see periodic (or at least regular) behavior for a given epoch, but the behavior changes from one epoch to the other. Observations taken between 1997 April 2 and April 16 show smooth variations (see Figure 9). During that period, the polarization was maximum at phase 0.1 and 0.7, whereas during the period from 1997 June 3 to July 11 (see Figure 10), a maximum in polarization was seen at phase 0.3 and a minimum at phase 0.0; the period we used,  $10.400 \pm 0.002$  d (Mathieu et al. 1989), is too well determined to allow shifts in phase, so a rearrangement must have occurred between the two sets of data, taken only 2 months apart. Figure 12 is the same as Figure 11 except that it includes data taken between 1998 April 27 and May 13; the added observations are all below the others. In this last figure, variations may not be as smooth as in Figure 9; variations in position angles are almost single-periodic with the exception of one point near phase 0.45. These sets of data from different epochs show different average polarization values and different polarization variations, which might indicate changes in the CS/CB environment for this star. This makes the accumulation of data over many years very noisy (compare the data for each epoch with Figure 8).

### 6.5. Haro 1-14C = HBC 644

This 591-day binary has an average polarization of 1.08% at  $34^\circ$  (Table 3). Data are presented in Table 13 and Figure 13, where one atypical observation is not shown. It is a suspected variable (Table 5 and Table 6). The average IS position angle of stars with the same distance modulus is  $24^\circ$ , similar to the observed position angle and indicative of IS polarization (see map in Figure 14). Since this star may be variable, we conclude that its polarization has a strong IS and a weaker intrinsic components.

### 6.6. NTTS 162814-2427 = ROX 42 or ROX 42C

NTTS 162814-2427 is a triple system, with a companion discovered by Lee (1992), at  $0''.15$  and position angle  $135^\circ$  (Ghez et al. 1993) and thus included in our measurements. The projected separation of the 35.95-day spectroscopic binary (Mathieu 1994) that has a mass ratio of  $1.09 \pm 0.07$  (Lee, Martín, & Mathieu 1994) is 0.27 AU, while the third star is at 19.4 AU (Jensen et al. 1996). This star has one of the most eccentric orbits. It also has a small UV excess, a small NIR excess and a weak  $H\alpha$  line with a P Cygni profile (Walter et al. 1994), which might indicate that there is more CS material than for other WTTS, but not enough to classify the star as CTTS. The shape of the  $H\alpha$  emission line changes with time, sometimes showing inverse P Cygni profile, which might be an indication of accretion processes (Mathieu 1992) with a low accretion rate. The age derived from the position in the HR diagram gives  $1 \times 10^6$  yr, which makes this binary one of the youngest yet found (Mathieu et al. 1989). Theoretical evolutionary models with different input physics have been investigated by Figueiredo (1997) who found that the observations for this binary are well

fitted by a  $1.10 M_{\odot}$  K4 primary, and a  $K5 1.00 M_{\odot}$  secondary, both with an age of  $3.7 \times 10^6$  yr. NTTS 162814-2427 was not detected at  $1100 \mu\text{m}$  (Skinner, Brown & Walter 1991), so an upper limit to the disk mass based on the  $3\sigma$  upper value of the  $1100 \mu\text{m}$  observations is  $0.11 M_{\odot}$ , although this star was observed under poor atmospheric conditions. There is a significant excess from the NIR up to  $60 \mu\text{m}$ , consistent with the presence of CB material (Walter et al. 1994)

Its SED is consistent with a CB disk in which the central region has been cleared (Jensen & Mathieu 1997). Using theoretical masses derived from evolutionary tracks and spectroscopic observations, Jensen & Mathieu (1997) find and use an inclination of  $71^{\circ}$ . The semi-major axis is then  $0.28 \text{ AU}$ , and the dynamically cleared gap goes from  $0.057$  to  $0.85 \text{ AU}$ . No silicate feature appears near  $10 \mu\text{m}$ . The SED modeling shows that there is no requirement that the disk be optically thin. The dynamical gap fits the data better than a continuous disk. The best fit gap is similar to the dynamical gap predicted by theory; the best fit is for  $0.047 \text{ AU}$  to  $0.40 \text{ AU}$ . The dynamical hole does not reproduce the observations well. But the model does not take into account the presence of the third star. The IR observations could be due to emission coming from the tertiary or its CS disk, without the need for disks around the primary and/or secondary stars. Also, the lack of submm emission could come from a cleared up CB disk, caused by interaction with the tertiary, and not from a gap in the CB disk.

The  $V$  magnitude varies up to  $0.4 \text{ mag}$  (Lee 1992 - reported by Jensen & Mathieu 1997). According to Zakirov et al. (1993), brightness variations in  $V$  had an amplitude of  $0.32 \text{ mag}$  in 1991/1992, with a rotational period of  $9.32\text{d}$ ; no eclipsing effect could be found. The similarity of the dynamical mass limits and the theoretical masses suggests that the inclination is small (Mathieu et al. 1989), but, as mentioned above, Jensen & Mathieu (1997) found an inclination of  $71^{\circ}$ .

NTTS 162814-2427 is at  $0.5^{\circ}$  from Haro 1-14C (see map in Figure 14). Its high polarization ( $3.5\%$  at  $22^{\circ}$ ) and high variability (see Tables 4, 5 and 6) indicate a large intrinsic polarization. The average IS position angle of stars with a similar distance modulus is  $25^{\circ}$ , close to NTTS 162814-2427's value and indicative of IS polarization. NTTS 162819-2423S has a polarization position angle close to that for NTTS 162814-2427, so this might indicate a local (intra-cluster) origin for part of the polarization of these two stars. We conclude that NTTS 162814-2427 has strong intrinsic polarization with a weaker IS component and possibly with a strong intra-cluster polarization.

Data are presented in Table 14 and Figures 15 and 16. The polarization has an average of  $3.5\%$  at  $22^{\circ}$  and is statistically variable. Two atypical observations are not included in the figures. The first one has a polarization almost  $1\%$  below the average, and a position angle of  $15^{\circ}$ . The second atypical observation also has a position angle of  $15^{\circ}$ , but its polarization level is only  $0.3\%$  below the average. These atypical measurements indicate some non-periodic change in this system. Subtraction of the IS component gives an intrinsic polarization of  $2.1\%$ , rather high for a WTTS or any PMS star. The presence of intrinsic polarization is in agreement with the evidences for CS material, but part of the intrinsic value could still be intra-cluster polarization. The fact that the amplitude of the polarimetric variations is very large, up to  $0.5\%$  (see Figure 15 and 16),

which is higher than for the other WTTS we observed, may also be supporting the indication that there is more CS material around NTTS 162814-2427 than for other WTTS. Alternatively, the high polarimetric variations may be due to the high eccentricity, or a favorable inclination. The binned data clearly show a periodic variation in position angle. In position angle and in  $U$ , the observations are strongly dominated by single-periodic variations; this might be a direct consequence of the orbital eccentricity, which is equal to 0.48. Strong single-periodic variations are here a consequence of orbital eccentricity, since the mass ratio is near unity and we have shown that in these cases, asymmetric CB envelopes do not produce single-periodic variations (Paper I).

### 6.7. NTTS 162819-2423S = ROX 43A

NTTS 162819-2423 is a quadruple system, with both components NTTS 162819-2423S (ROX 43A) and NTTS 162819-2423N (ROX 43B) themselves binary stars. The projected separation of the 89.1-day spectroscopic binary (Mathieu 1994) (south component) is 0.10 AU, whereas the binary in the north component has a projected separation of 2 AU and both binary systems are separated by 600 AU (projected) (Jensen et al. 1996). NTTS 162819-2423N is about 1 mag fainter in  $V$  than the southern component (Mathieu et al. 1989) and  $4''.8$  away (Simon, Ghez, & Leinert 1993). According to Zakirov et al. (1993), brightness variations in  $V$  had a small amplitude of 0.1 mag in 1991/1992, with a rotational period of roughly 3.2 d; no eclipsing effect could be found.

NTTS 162819-2423S was not detected at  $1100 \mu\text{m}$  (Skinner et al. 1991), so an upper limit to the disk mass based on the  $3\sigma$  upper value of the  $1100 \mu\text{m}$  observations is  $0.12 M_{\odot}$ , although this star was observed under poor atmospheric conditions. There is a large NIR excess (Walter et al. 1994) suggesting the presence of dust somewhere in this system. Jensen & Mathieu (1997) argue that the excess emission at  $60 \mu\text{m}$  suggests the presence of material outside the binary orbit in a CB disk. Its SED is consistent with a CB disk in which the central region has been cleared (Jensen & Mathieu 1997). With the mass function, inclinations lower than  $22^{\circ}$  would give a secondary mass higher than that of the primary, which is unlikely (Jensen & Mathieu 1997) so probably  $i > 22^{\circ}$ . S has a prominent  $10 \mu\text{m}$  silicate emission feature, which is reproduced with an optically thin inner disk. The continuous disk does not reproduce the observations well. A gap or hole fit the data, but neither does so perfectly (Jensen & Mathieu 1997).

Data are presented in Table 15 and Figure 17. The average polarization, 2.92% at  $16^{\circ}$ , is statistically variable. NTTS 162819-2423S is  $0.5^{\circ}$  distant from Haro 1-14C and  $0.1^{\circ}$  from the previous star (see map in Figure 14). It has a lower polarization than the last star, with 2.9% average polarization at  $16^{\circ}$ . Since it is polarimetrically variable, it has an intrinsic polarization, but the IS one dominates; there might also be an intra-cluster component. Since we used a  $8''.2$  aperture hole, it is not impossible that some observations accidentally included more than just the southern binary. We have made some tests using different aperture holes and conclude that when the North and South components are included in the measurements, the polarization is higher by  $\approx 0.2\%$ . That may explain the chaotic polarimetric observations that show wild fluctuations in

polarization; nonetheless, some of the variations could be attributed to the orbital motion of the southern component alone. Future polarimetric observations should be made with much smaller aperture holes, making sure what is included in the measurement.

## 7. Orbital inclination

One of the goals of these polarimetric observations is to determine the orbital inclinations of the selected PMS binaries, by using the BME formalism. This formalism can still be used if the orbits are non-circular and the scatterers are spherical grains, within the limits presented in Papers I and II.

Noise with a standard deviation greater than 10% of the amplitude of the polarimetric variations will prevent the BME formalism from finding a reasonable estimate of the true inclination (Paper I). Other studies have also shown that the quality of the data (number of data points, observational errors, amplitude of the polarimetric variations) can also strongly influence the results found by the BME formalism.

Aspin, Simmons, & Brown (1981) have studied the standard deviation  $\sigma_{\text{nec}}(i)$  which is necessary to determine an inclination  $i$  to  $\approx \pm 5^\circ$ , with a 90% confidence level. They give an approximate relation for the data quality  $DQ$ :

$$DQ = \frac{\sigma_o}{A_o \sqrt{N_o}} = \frac{\sigma_{\text{nec}}(i)}{A(i) \sqrt{N}}, \quad (5)$$

where

$$A = \frac{|Q_{\text{max}} - Q_{\text{min}}| + |U_{\text{max}} - U_{\text{min}}|}{4}, \quad (6)$$

$\sigma_o$  is the observational error of the polarization,  $A_o$  is the observed polarimetric variability calculated with Equation 6,  $N_o$  is the number of observations, and  $N = 40$  (the number of bins in their simulations). A set of very good quality observations will have a low value of  $DQ$ . We present in Table 16, Column 2,  $DQ$  values for the binaries studied here. After the quantity  $\sigma_{\text{nec}}(i)/A(i)$  is calculated, Table 1 in Aspin et al. (1981) gives the lowest possible inclination that can be determined from the observations with a  $\pm 5^\circ$  accuracy at a significance of 10% (meaning that the true inclination has a probability of 90% to be within  $\pm 5^\circ$  of the value returned by the BME formalism). If we apply this method to our sets of data, we find that the quality of our data do not allow us to find  $i$  to  $\approx \pm 5^\circ$ , with a 90% confidence level, for any of our binaries.

Wolinski & Dolan (1994) have also studied the confidence intervals for orbital parameters determined polarimetrically. They made Monte Carlo simulations of noisy polarimetric observations, for a specific geometry not suitable for the stars studied in this present paper, but their results are nonetheless instructive. Confidence intervals for  $i$  are given graphically as a function of a “figure

of merit”  $\gamma$ :

$$\gamma = \left(\frac{A}{\sigma_p}\right)^2 \left(\frac{N}{2}\right), \quad (7)$$

where  $\sigma_p$  is the standard deviation of the noise that was added to the data,  $N$  is the number of observations, and  $A$  is still given by Eq. 6. We have calculated and present in Column 3 of Table 16 the figures of merit  $\gamma$  for some PMS binaries, by using the observational error  $\sigma(P)$  instead of the  $\sigma_p$  used by Wolinski & Dolan. It is again seen that the quality of the data is not very good, mostly because the amplitude  $A$  is rather low (between 0.02 and 0.10% in general).

Finally, following our own studies of the effects of noise on the BME results (Paper I), we have calculated the noise for the Stokes parameters  $Q$  and  $U$ , by using the variance of the fit and the amplitude of the polarimetric variations; these amplitudes are computed from the maximum and minimum values of the observations, and not those of the fit. These calculations are presented in Columns 4 and 5 of Table 16, where levels of noise below 10% are non-existent. Once again, this analysis shows that the polarimetric observations of PMS stars are not of “very good quality”, not because of instrumental or observational problems, but because non-periodic stochastic polarization variations and low-amplitude periodic variations make the data rather noisy, hiding whatever periodic polarimetric variations exist. Future observations should be obtained at a site offering many consecutive clear nights to cover in one run the whole orbital period.

A more interesting case will be presented in a future paper (Manset & Bastien, in preparation). AK Sco was observed within a few (12) consecutive nights, and shows polarimetric variations of greater amplitude.

Assuming the BME formalism can be used to analyze the polarimetric variations of binary PMS stars, we have added in Table 16 the results of the BME analysis for the orbital inclination. Most of the inclinations are near  $90^\circ$ , which cannot be a real result. This is compatible with the above discussion on the effects of the stochastic noise on the inclination analysis.

## 8. Orientation of the orbital plane and moments of the distribution of the scatterers

In addition to the orbital inclination, the BME formalism returns  $\Omega$ , the orientation of the orbital plane with respect to the plane of the sky, and moments of the distribution of the scatterers which are used to measure the asymmetry with respect to the orbital plane ( $\tau_0 G$ ), and the degree of concentration towards the orbital plane ( $\tau_0 H$ ). It is generally expected that the distribution will be symmetrical to and concentrated in the orbital plane, so  $\tau_0 H > \tau_0 G$ . In Table 17, we present the values of  $\Omega$ ,  $\tau_0 H$ ,  $\tau_0 G$ , and the ratio  $\tau_0 H/\tau_0 G$ . If the circumbinary disks of these binaries can be imaged (with interferometric or adaptive optics techniques), their orientation should be similar to  $\Omega$ , although the orbits are not necessarily coplanar with the disks or envelopes. The values for  $\tau_0 G$  and  $\tau_0 H$  are similar to those we have found in numerical simulations (Paper I), and to the observed values for other types of binaries (Bastien 1988; Koch, Perry, & Kilambi 1989). In



particular,  $\tau_0 H > \tau_0 G$  as expected, with ratios approximately from 1.0 to 3.5.

These parameters are also calculated using the coefficients of the fits and the same assumptions (the scatterers are electrons, the orbits are circular). However, single-periodic variations that are not present when the scatterers are electrons and the orbits are circular, do appear in our simulations when there are dust grains instead of electrons, when variable optical depth effects are considered, or when the orbits are eccentric (Papers I and II). Therefore, the values of the parameters calculated might not reflect an asymmetric configuration ( $\tau_0 G$ ) or a concentration toward the orbital plane ( $\tau_0 H$ ). For example, we have found, using the code presented in Papers I and II, that even though  $\tau_0 G$  should be null for a perfectly symmetric configuration, it will not be so if we have dust grains or consider variable optical depth effects.

## 9. Search for Correlations

To study correlations between variations and orbital parameters (period and eccentricity), the maximum and minimum values (excluding the atypical observations) were used to calculate  $\Delta P$ ,  $\Delta\theta$ ,  $\Delta Q$ ,  $\Delta U$ , and  $(\Delta Q + \Delta U)$  for all the binaries of this study), and compare them to the orbital period and eccentricity; see Table 4, Figures 18, 19, and 20. Note that in these figures, the quantity  $\Delta\theta$  for some stars is not meaningful since their polarizations are very low, and hence, their position angles not well defined. There are no clear correlations between the polarimetric variations and the orbital characteristics, although the most variable PMS binaries have intermediate periods (10–100 d) and intermediate eccentricities (0.3–0.5). The converse is not true, and there are examples of binaries with intermediate period or eccentricity which do not present high variations. One should not forget, however, that orbital inclination strongly affects the variability; a binary which should display a high level of variability because of, say, its orbital eccentricity, might not do so because its orbital inclination is masking the variations.

Important variability for long orbital periods is not expected, since the angular dimension of the CS disk as seen by the other star decreases as distance increases, making the variations in scattering angles smaller, and thus the polarimetric variations themselves smaller; this has been verified using the numerical codes presented in Papers I and II. Moreover, the long-period binaries with periods over  $\approx 100$  d have probably not been adequately sampled to assess the polarimetric variability over a full orbit. These two reasons could explain the drop in variability for periods longer than about 100 d. The most variable binaries all have high orbital eccentricities,  $e > 0.3$ . The 2 stars with high eccentricity but low-amplitude variations, Haro 1-14C and NTTS 045251+3016, also have long periods (591 and 2530 d respectively), which might explain why more variability is not seen.

Correlation between polarimetric properties and stellar age is difficult to study because many factors introduce uncertainties in the derived ages. First, the presence of unresolved companions, which increases the total luminosity, can artificially lower the derived age (Simon et al. 1993).

Second, the choice of evolutionary tracks affects the estimated ages, as well as uncertainties in extinction or distance (Walter et al. 1994; Forestini 1994; D’Antona & Mazzitelli 1994). Third, Hartmann et al. (1991) have suggested that prolonged disk accretion can arrest the evolution so the true age is greater than the one found by the location of a star in the HR diagram. So a binary can have a low polarization because it is old and has lost its CS material, or because it is still young but did not have much material to accrete due to an earlier SN explosion for example. This discussion also does not take into account the effects of inclination on the level of polarization. We could look for correlations for binaries whose age are derived from the same evolutionary tracks, but since many other factors influence the polarization level, we have not tried to do so.

Our numerical simulations show that, as the orbital eccentricity increases, variations go from being double-periodic (seen twice per orbit) to being single-periodic (seen only once per orbit). Therefore, as  $e$  increases, the ratio of single-periodic over double-periodic variations ( $1\lambda/2\lambda$ ) should start from zero and increase. However, the inclination also plays a role in the amplitude of the variations and can decrease them. Table 18 and Figure 21 show this ratio for  $P$ ,  $\theta$ ,  $Q$ , and  $U$ , and all the binaries we have studied. No correlation is seen, although this might be due to the presence of noise in the observations. One of the highest-eccentricity binaries, NTTS 162814-2427 ( $e=0.48$ ) does present strong single-periodic variations in  $\theta$  and  $U$ , which is consistent with the results of our numerical simulations. Other factors, though, can produce single-periodic variations: geometry, variable absorption effects.

## 10. Discussion and summary

We have presented polarimetric observations obtained at  $7660\text{\AA}$  and  $5550\text{\AA}$  for 7 spectroscopic PMS binaries located in the  $\rho$  Oph and Upper Sco star forming regions (SFRs). All binaries have detectable linear polarizations and most are significantly affected by interstellar (IS) polarization. NTTS 162814-2427 and NTTS 162819-2423S have high intrinsic polarization and are  $0.2$  from one another (0.22 pc at a distance of 125 pc), so intra-cluster or very localized polarization might also contribute to the observations. Since it does not affect Haro 1-14C located  $0.5$  away (see below), this localized polarization would affect about 1 pc around NTTS 162814-2427 and NTTS 162819-2423S. After an estimate of this IS polarization is removed, all binaries present intrinsic polarizations  $\gtrsim 0.4\%$  at  $7660\text{\AA}$ . Two binaries which, based on their SED and in particular their NIR excesses, have detectable amounts of dust, NTTS 162814-2427 and NTTS 162819-2423S, also have the highest intrinsic polarization ( $\approx 1.5\text{--}2.1\%$ ), which might include some intra-cluster polarization. The amplitudes of their variations (0.5–1.0%) also indicate strong intrinsic polarizations.

Of the 22 T Tauri and Herbig Ae/Be binaries studied so far (Papers III and IV, this paper), 68% (15/22) have intrinsic polarization above 0.5% at  $7660\text{\AA}$ . Many of those binaries do not present any evidence other than polarimetric for the presence of dust, indicating that polarimetric techniques are more sensitive to the presence of dust than photometric or spectroscopic ones. Most of the binaries with intrinsic polarizations below 0.5% are located in the Tau, Aur, Ori SFRs, suggesting

that these regions might be older than the Sco and Oph ones.

All binaries located in the Sco and Oph SFRs are statistically variable or possibly variable. When considering the binaries previously studied in Papers III and IV, and for which we have enough observations, including data from the literature ( $N=21$ ), 53% (11/21) are clearly variable, and 90% (19/21) are variable or possibly so. These numbers include variability seen in the periodic variations but not detected by the statistical tests, and agree with results for single stars (Bastien 1988, Ménard & Bastien 1992). All the known CTTS binaries in our sample (except DQ Tau for which we only have one measurement) and many NTTS and WTTS present polarimetric variations.

Three stars of the Oph and Sco SFRs have shown, twice, and at  $7660\text{\AA}$  atypical values of polarization and/or position angle that are well below or above the rest of the data (NTTS 155913-2233, NTTS 162814-2427, NTTS 160905-1859). These atypical observations were also detected in our previous samples (Par 1540, Par 2494, and MWC 1080). We believe these are real observations of events that strongly affected the stars and/or their environment. For the stars with a sufficient amount of data, additional observations at similar phases indicate that these atypical points are not related to the normal periodic behavior. Interestingly, in the Sco and Oph sample, only the shortest period binaries ( $< 36$  d) have shown these atypical observations; the other 2 cases, with periods of 89 and 144 d, did not show any such atypical observations. Although atypical observations could possibly be detected with more observations, this might indicate that the atypical observations are caused by the close proximity of the stars, in particular, the interaction between their CS disks.

A few of the PMS binaries present periodic polarimetric variations, despite the noise introduced by non-periodic or pseudo-periodic variations. Statistical tests conclude that NTTS 155913-2233's polarization is possibly variable, and low-amplitude periodic variations are seen when the data at  $7660\text{\AA}$  are binned to minimize the noise. NTTS 160814-1857 presents clear periodic and phased-locked variations with an amplitude of 0.2% over  $\sim 10$  orbits, and has not shown any atypical observations, pointing to long-term stability. This might be due to the period of 144.7 days, which keeps the stars and their CS disks apart despite the relatively high eccentricity (0.26). NTTS 160905-1859 presents periodic but not phased-locked variations. No periodic variation is seen when viewing all the data, but more regular variations are seen when taking shorter time intervals that include only a few orbits at a time. This points to rapid re-arrangement of the CS material, on a time scale of 1 orbit, and might also explain 2 atypical observations. NTTS 162814-2427 presents very variable and noisy polarization with an amplitude of 0.6%. Whereas the variations as usually seen in polarization, NTTS 162814-2427's variations are clear in position angle, although with a low amplitude of less than  $3^\circ$ . Moreover, the variations in position angle are mostly single-periodic (seen once per orbit), which might be the result of the high eccentricity 0.48, as predicted by our numerical simulations (Papers I and II). NTTS 162819-2423S presents high amplitude (1%) polarimetric variations, but those are very noisy. This might be due to the quadruple nature of this system, and the accidental inclusion of more than the South binary in some of the measurements. The amplitude of the periodic polarimetric variations is greater in the Sco and Oph sample (0.2 – 1.2%) than in the Tau, Aur, Ori one ( $\lesssim 0.3\%$ ). Additional polarimetric observations obtained over a

shorter period of time would be interesting to see if the noise is reduced and the variations hence made clearer, and if the variations are still periodic.

One of the goals of these observations was to find the orbital inclinations. Unfortunately, non-periodic or pseudo-periodic variations sometimes mask the truly periodic variations by introducing noise. This noise is too high for the BME formalism to find reasonable estimates of the orbital inclination, in the 22 binaries studied so far. Three factors contribute to this difficulty. First, dust grains are the main scatterers in these systems, and it has been shown that dust grains produce polarimetric variations of smaller amplitude than electrons (Paper II). Second, the disk around these short-period binaries are probably CB rather than CS ones, and CB disks produce variations of smaller amplitudes than CS disks (Paper II). Finally, non-periodic events introduce noise that mask the already small amplitude variations. This last problem might be improved by taking data on shorter periods of time.

The BME formalism also returns moments of the distribution of the scatterers, used to measure the asymmetry with respect to the orbital plane and the degree of concentration towards the orbital plane. Although the assumptions used in the BME formalism (scattering on electrons, circular orbits) are not met in the PMS binaries studied here, the values returned for PMS binaries are of the same order of magnitude as values for other types of stars and as for our simulations ( $\sim 1-10 \times 10^{-4}$ ).

There are no clear correlations between the polarimetric variations and the orbital characteristics. The most variable binaries all have high orbital eccentricities,  $e > 0.3$ . The 2 stars with high eccentricity but low amplitude variations, Haro 1-14C and NTTS 045251+3016, also have long periods, which might explain why more variability is not seen.

N. M. thanks the directors of the Mont Mégantic Observatory for granting generous time over many years. The technical support from the technicians of the observatory, B. Malenfant, G. Turcotte, and F. Urbain is duly acknowledged. N. M. thanks the Conseil de Recherche en Sciences Naturelles et Génie of Canada, the Fonds pour la Formation de Chercheurs et l'Aide à la Recherche of the province of Québec, the Faculté des Etudes Supérieures and the Département de physique of Université de Montréal for scholarships, and P. B. for financial support. We thank the Conseil de Recherche en Sciences Naturelles et Génie of Canada for supporting this research. We thank François Ménard for providing the Pic-du-Midi data. N. M. is Guest User, Canadian Astronomy Data Centre, which is operated by the National Research Council, Herzberg Institute of Astrophysics, Dominion Astrophysical Observatory.

## REFERENCES

- Adams, N. R., Walter, F. M., & Wolk, S. J. 1998, *AJ*, 116, 237
- Aspin, C., Simmons, J. F. L., & Brown, J. C. 1981, *MNRAS*, 194, 283
- Bastien, P. 1982, *A&AS*, 48, 153
- Bastien, P. 1988, in *Polarized Radiation of Circumstellar Origin*, ed. G. V. Coyne et al. (Tucson, AZ: University of Arizona Press), 595
- Bastien, P. 1996, in *ASP Conf. Ser. 97, Polarimetry in the Interstellar Medium*, ed. W. G. Roberge & D. C. B. Whittet (San Francisco: ASP), 297
- Bouvier, J., Cabrit, S., Fernández, M., Martín, E. L., & Matthews, J. M. 1993, *A&A*, 272, 176
- Brown, J. C., Mclean, I. S., & Emslie, A. G. 1978, *A&A*, 68, 415
- D’Antona, F., & Mazzitelli, I. 1994, *ApJ Suppl. Series*, 90, 467
- Drissen, L., Bastien, P., & St-Louis, N. 1989, *AJ*, 97, 814
- Figueiredo, J. 1997, *A&A*, 318, 783
- Forestini, M. 1994, *A&A*, 285, 473
- Ghez, A., Neugebauer, G., & Matthews, K. 1993, *AJ*, 106, 2005
- Hartmann, L., Jones, B. F., Stauffer, J. R., & Kenyon, S. J. 1991, *AJ*, 101, 1050
- Heiles, C. 2000, *AJ*, 119, 923
- Herbig, G. H., & Bell, K. R. 1988, *Lick Obs. Bull.* 1111, 1
- Herbst, W. 1989, *AJ*, 98, 2268
- Jensen, E. L. N., & Mathieu, R. D. 1997, *AJ*, 114, 301
- Jensen, E. L., Mathieu, R. D., & Fuller, G. A. 1996, *ApJ*, 458, 312
- Koch, R. H., Perry, P. M., & Kilambi, G. C. 1994, *IAU Information Bulletin on Variable stars*, no 4032
- Lee, C. W. 1992, Ph.D. thesis, University of Wisconsin
- Lee, C. W., Martín, E. L., & Mathieu, R. D. 1994, *AJ*, 108, 1445
- Manset, N. 2000, Ph.D. thesis, Université de Montréal
- Manset, N., & Bastien, P. 1995, *PASP*, 107, 483

- Manset, N., & Bastien, P. 2000, *AJ*, 120, 413 (Paper I)
- Manset, N., & Bastien, P. 2001a, *AJ*, 122, 2692 (Paper II)
- Manset, N., & Bastien, P. 2001b, *AJ*, 122, 3453 (Paper III)
- Manset, N., & Bastien, P. 2002, *AJ*, 124, 1089 (Paper IV)
- Mathewson, D. S., Ford, V. I., Klare, G., Neckel, TH., & Krautter, J. 1978, *BICDS*, 14, 115
- Mathieu, R. D. 1992, *Evolutionary Processes in Interacting Binaries*, edited by Y. Kondo, pp. 21-30
- Mathieu, R. D. 1994, *ARA&A*, 32, 465
- Mathieu, R. D., Walter, F. M., & Myers, P. C. 1989, *AJ*, 98, 987
- Ménard, F., & Bastien, P. 1992, *AJ*, 103, 564
- Prato, L., & Simon, M. 1996, *BAAS*, 189, 4907
- Press, W. H., Teukolsky, S. A., Vetterling, W. T., & Flannery, B. P. 1997, *Numerical Recipes in C, The Art of Scientific Computing*, 2d edition (Cambridge: Cambridge University Press)
- Robert, C., Moffat, A. F. J., Bastien, P., St-Louis, N., & Drissen, L. 1990, *ApJ*, 359, 211
- Robert, C., et al. 1992, *ApJ*, 397, 277
- Rudy, R. J., & Kemp, J. C. 1978, *ApJ*, 221, 200
- Simon, M., Ghez, A. M., & Leinert, Ch. 1993, *ApJ*, 408, 33
- Skinner, S. L., Brown, A., & Walter, F. M. 1991, *AJ*, 102, 1742
- Stellingwerf, R. F. 1978, *ApJ*, 224, 953
- Walter, F. M. 1986, *ApJ*, 306, 573
- Walter, F. M., Vrba, F. J., Mathieu, R. D., Brown, A., & Myers, P. C. 1994, *AJ*, 107, 692
- Wolinski, K. G., & Dolan, J. F. 1994, *MNRAS*, 267, 5
- Zakirov, M. M., Azimov, A. A., & Grankin, K. N. 1993, *IAU Information Bulletin on Variable stars*, no 3898

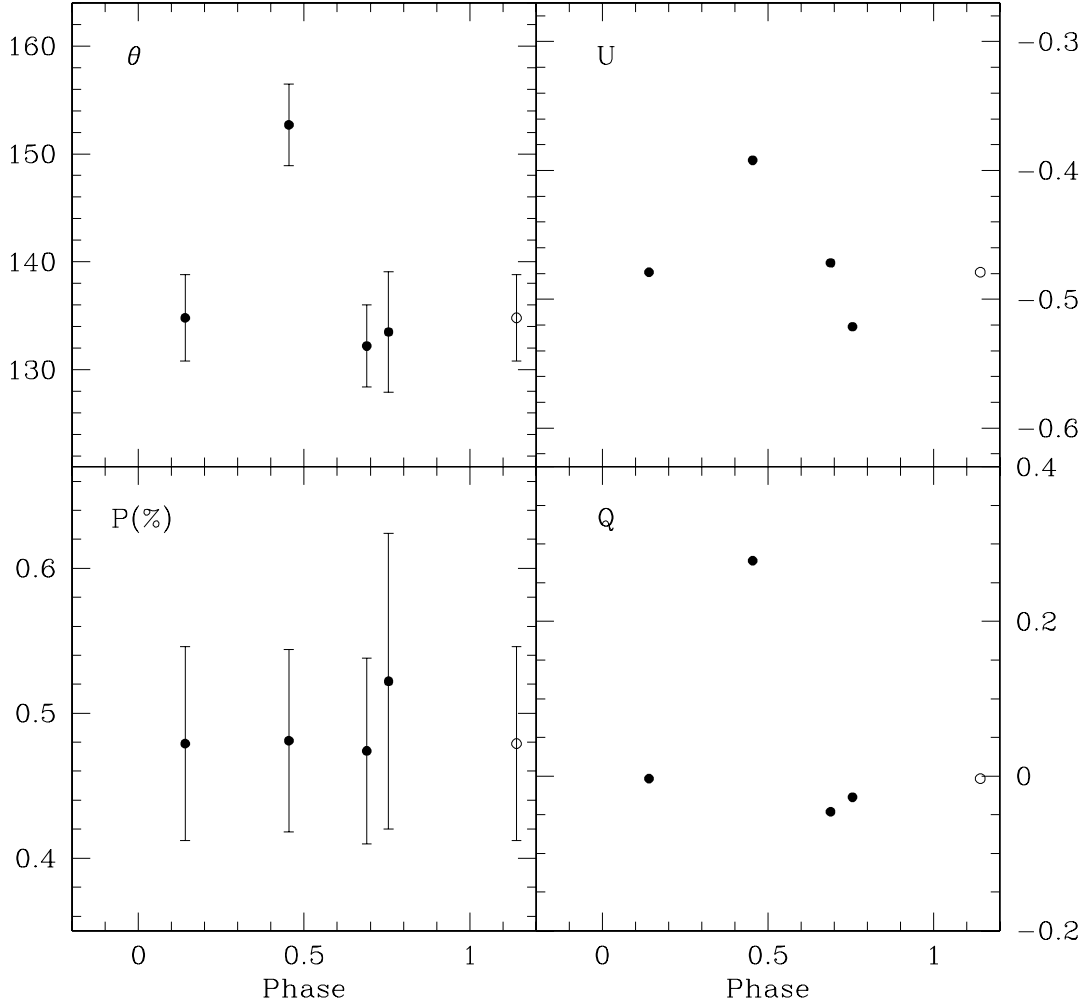


Fig. 1.— Polarimetric observations of NTTS 155808-2219. The polarization  $P$ , its position angle  $\theta$ , and the Stokes parameters  $Q = P \cos 2\theta$  and  $U = P \sin 2\theta$  are graphed as functions of the orbital phase.

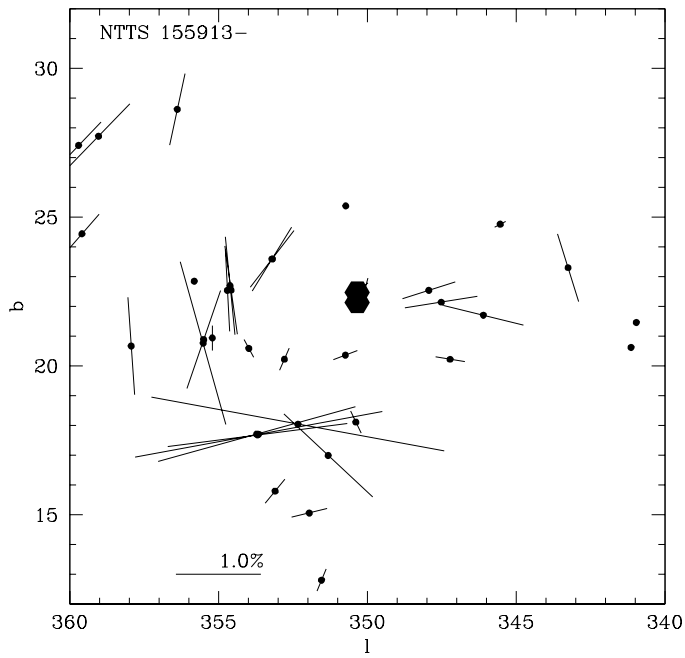


Fig. 2.— Map of the interstellar polarization in the vicinity of NTTS 155913-2233 (hexagonal symbol at the center of the map) and NTTS 155808-2219 (above center). The stars selected to calculate the IS polarization are within 80 pc of those targets.



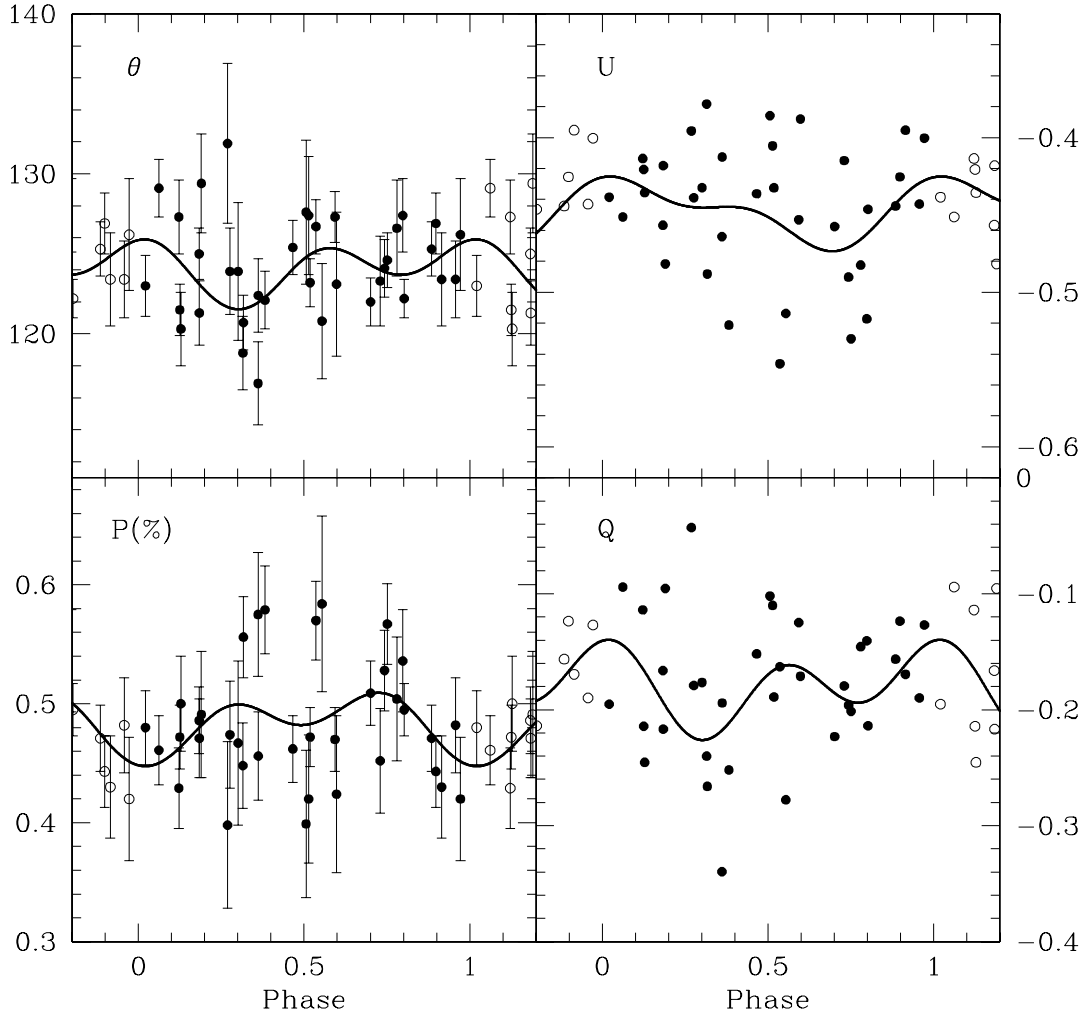


Fig. 3.— Polarimetric observations of NTTS 155913-2233. The star is variable polarimetrically, but there is a lot of scatter and no clear periodic variations. Two atypical observations, taken in 1995 May and 1997 April are not shown since their position angle,  $162^\circ$  and  $168^\circ$ , are very different from the rest of the observations.

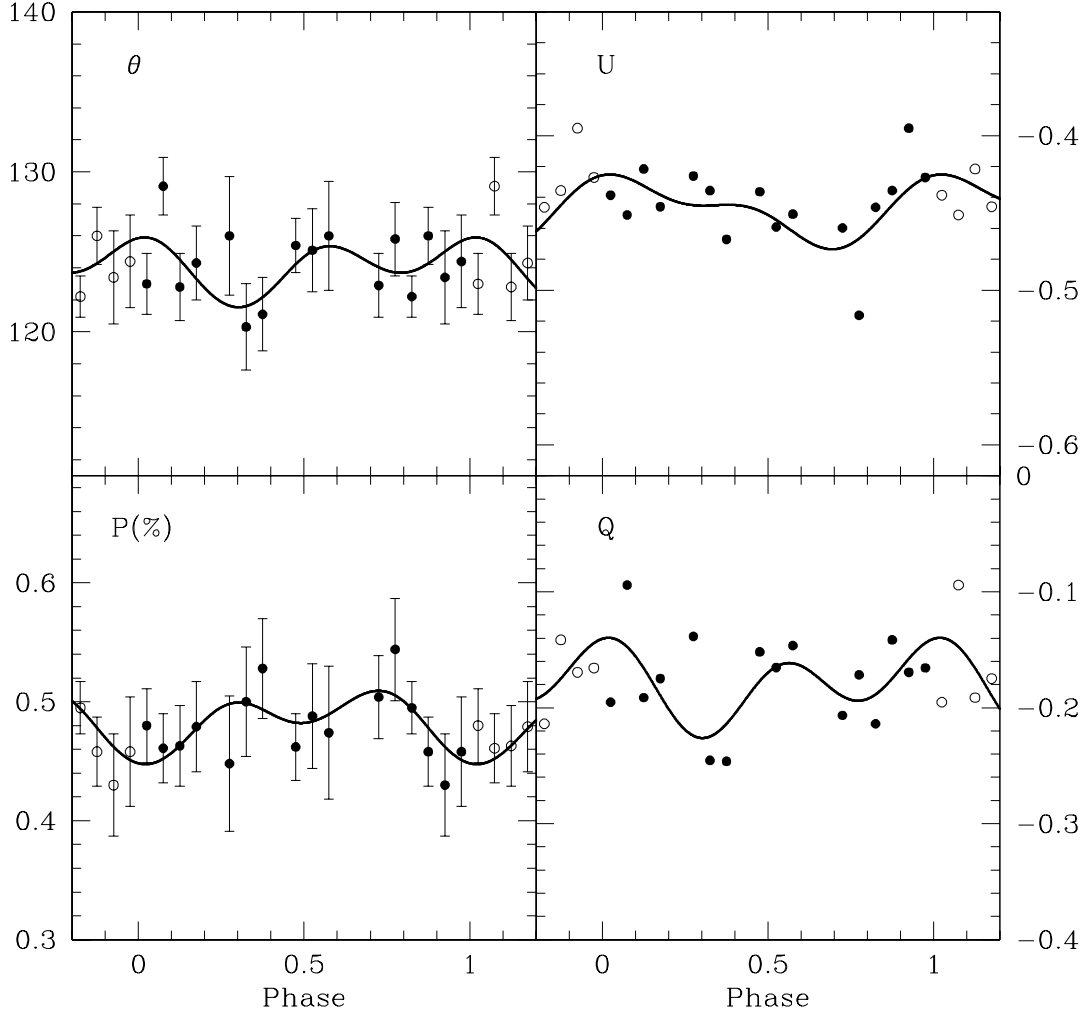


Fig. 4.— Binned polarimetric observations of NTT 155913-2233; if there are periodic polarimetric variations, they are of very small amplitude.

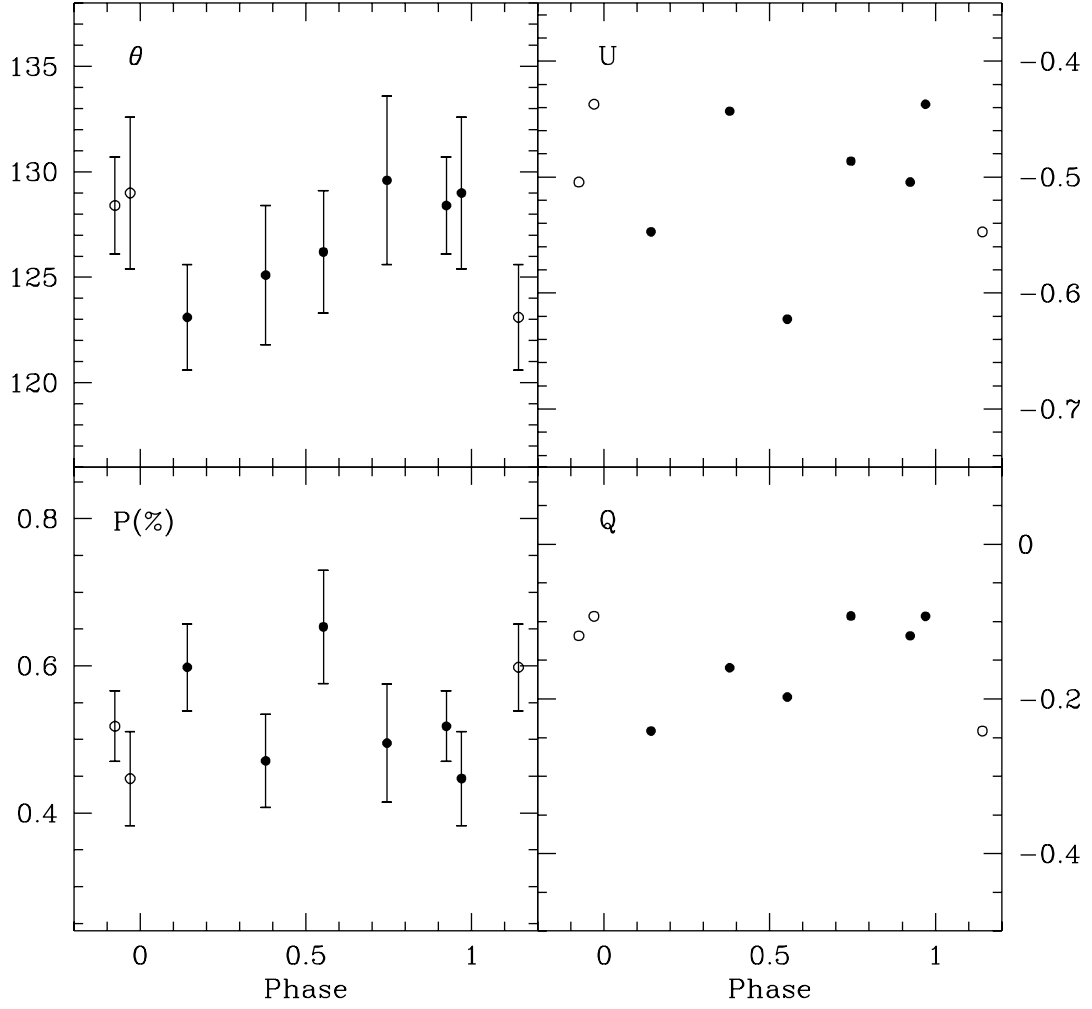


Fig. 5.— Polarimetric observations for NTTS 155913-2233 obtained at  $5550\text{\AA}$ . The position angle exhibits a systematic variation.

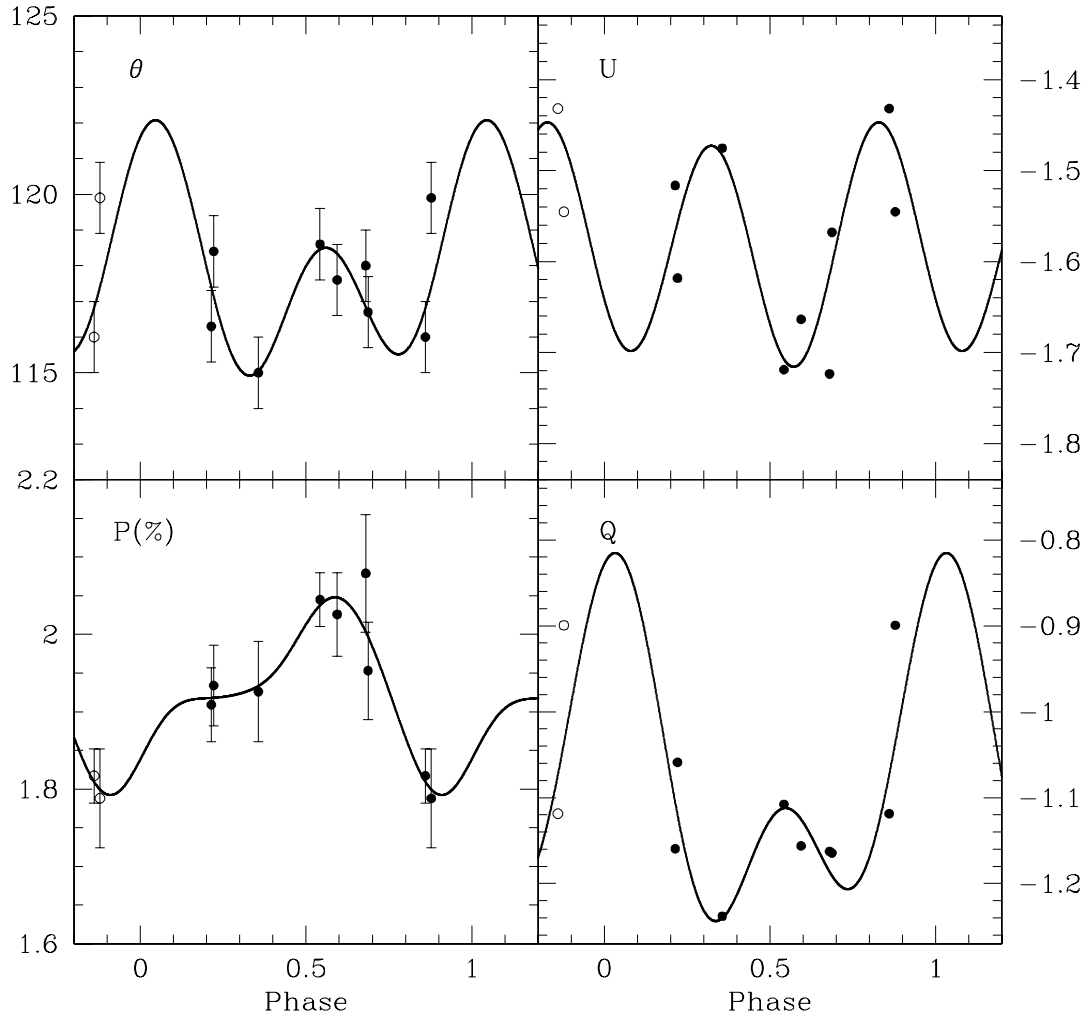


Fig. 6.— Polarimetric observations of NTTS 160814-1857.

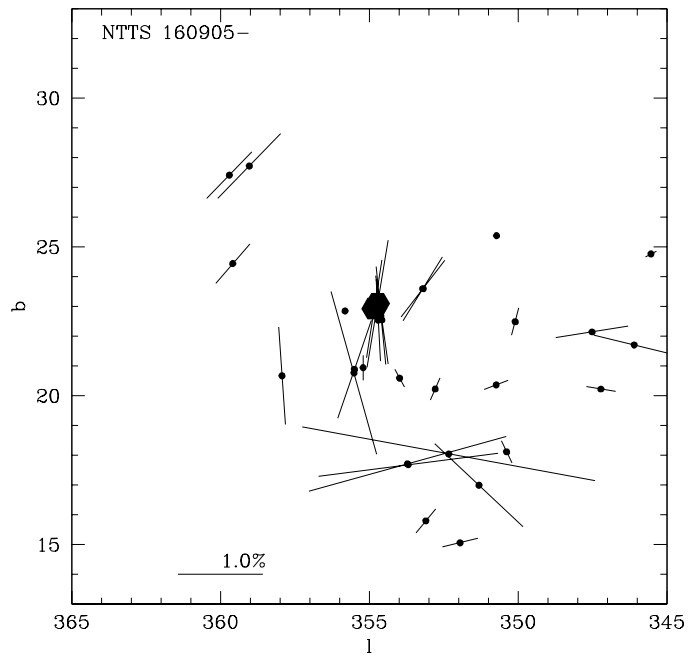


Fig. 7.— Map of the interstellar polarization in the vicinity of NTTS 160905-1859 and NTTS 160814-1857 (both at the center of the map). The stars selected to calculate the IS polarization are within 75 pc of those targets.

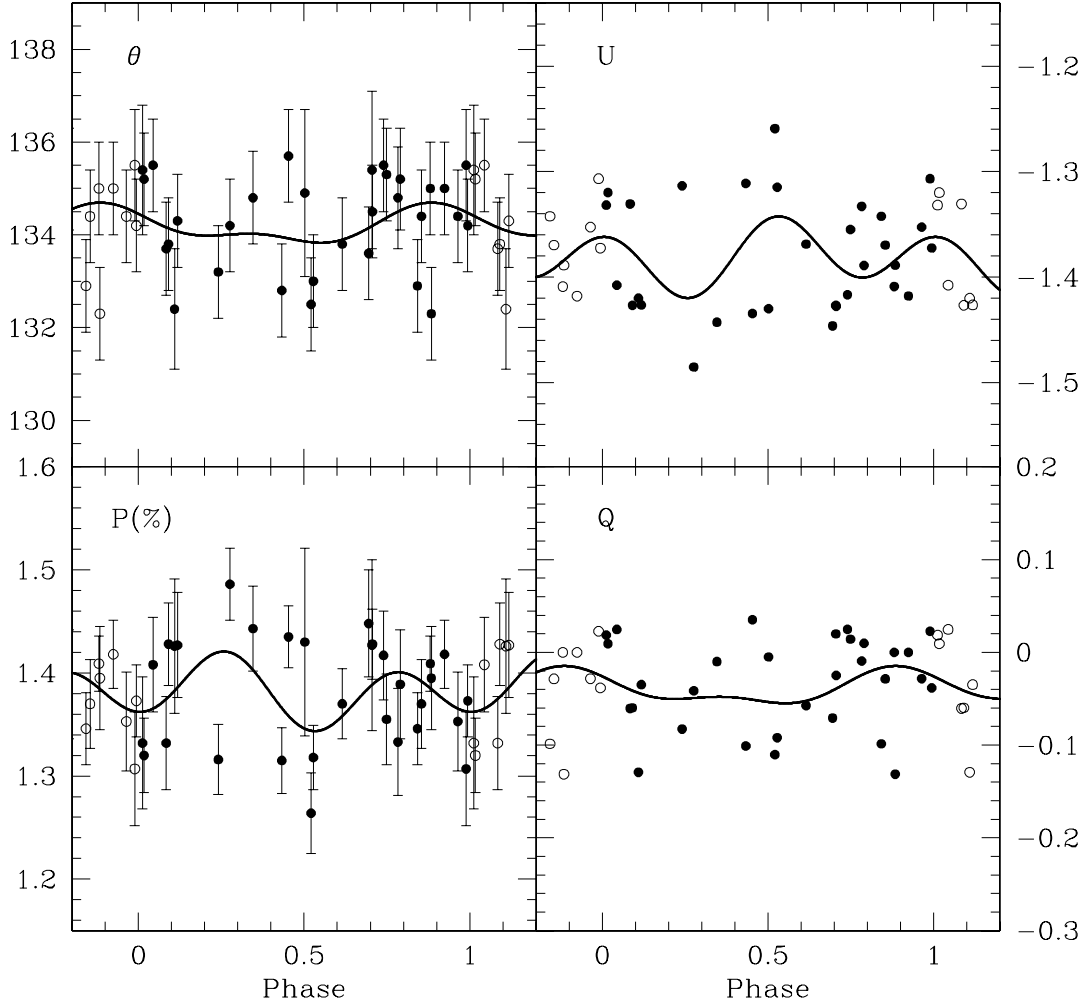


Fig. 8.— Polarimetric observations of NTTS 160905-1859 that show a lot of scatter. Two atypical observations, taken in 1996 May and 1998 May, were removed since their position angle was much lower or higher than the rest of the observations.

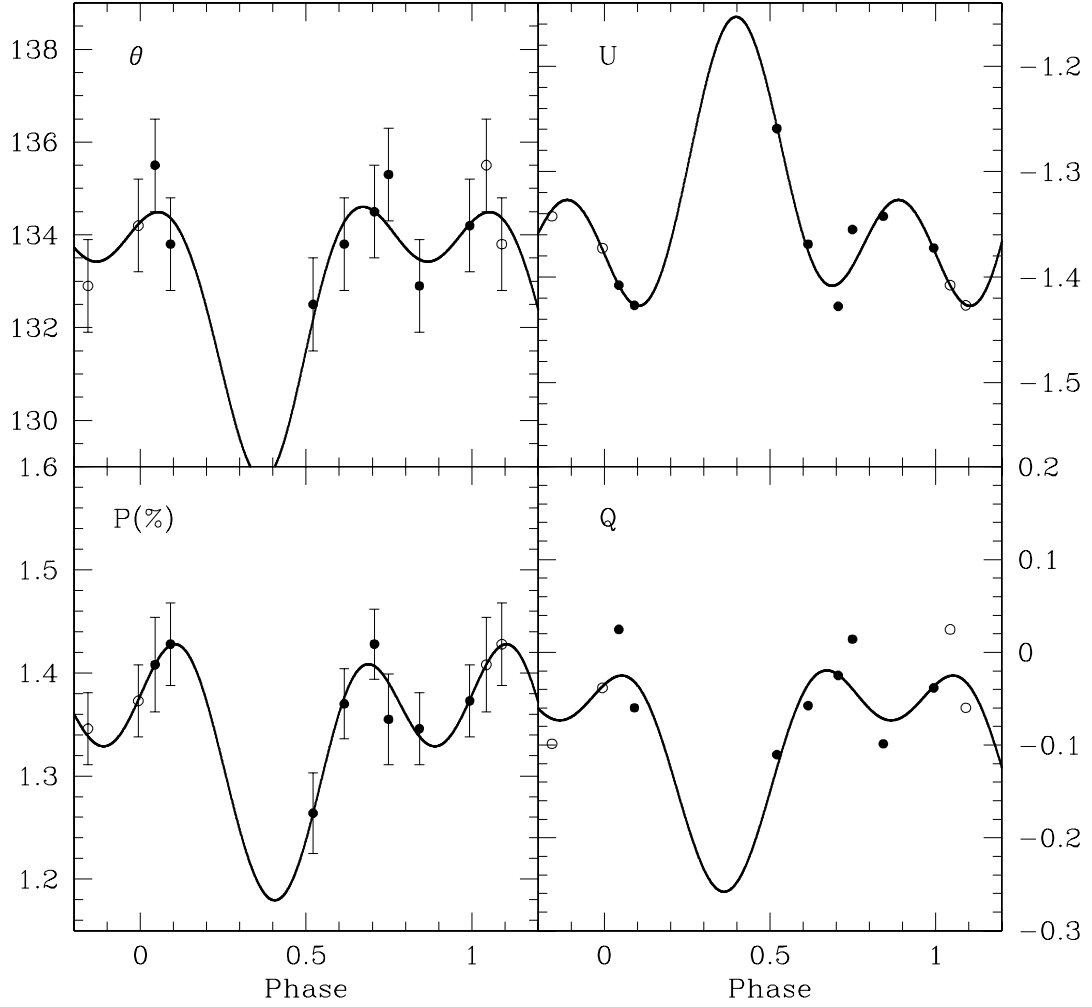


Fig. 9.— Subset of the the polarimetric observations of NTT 160905-1859, obtained between 1997 April 2 and 1997 April 16.

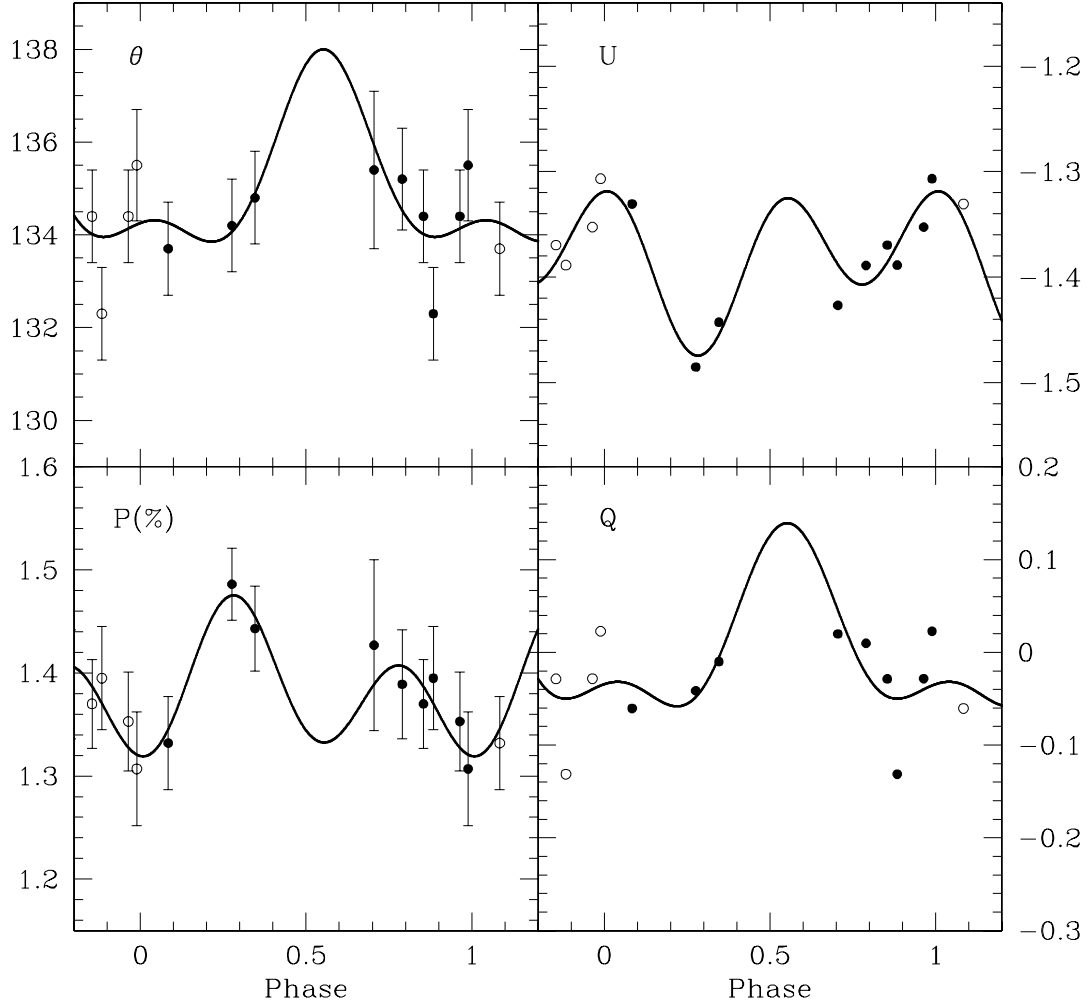


Fig. 10.— Subset of the polarimetric observations of NTTS 160905-1859 obtained between 1997 June 3 and July 11. The behavior is clearly different from the one presented in the preceding figure.



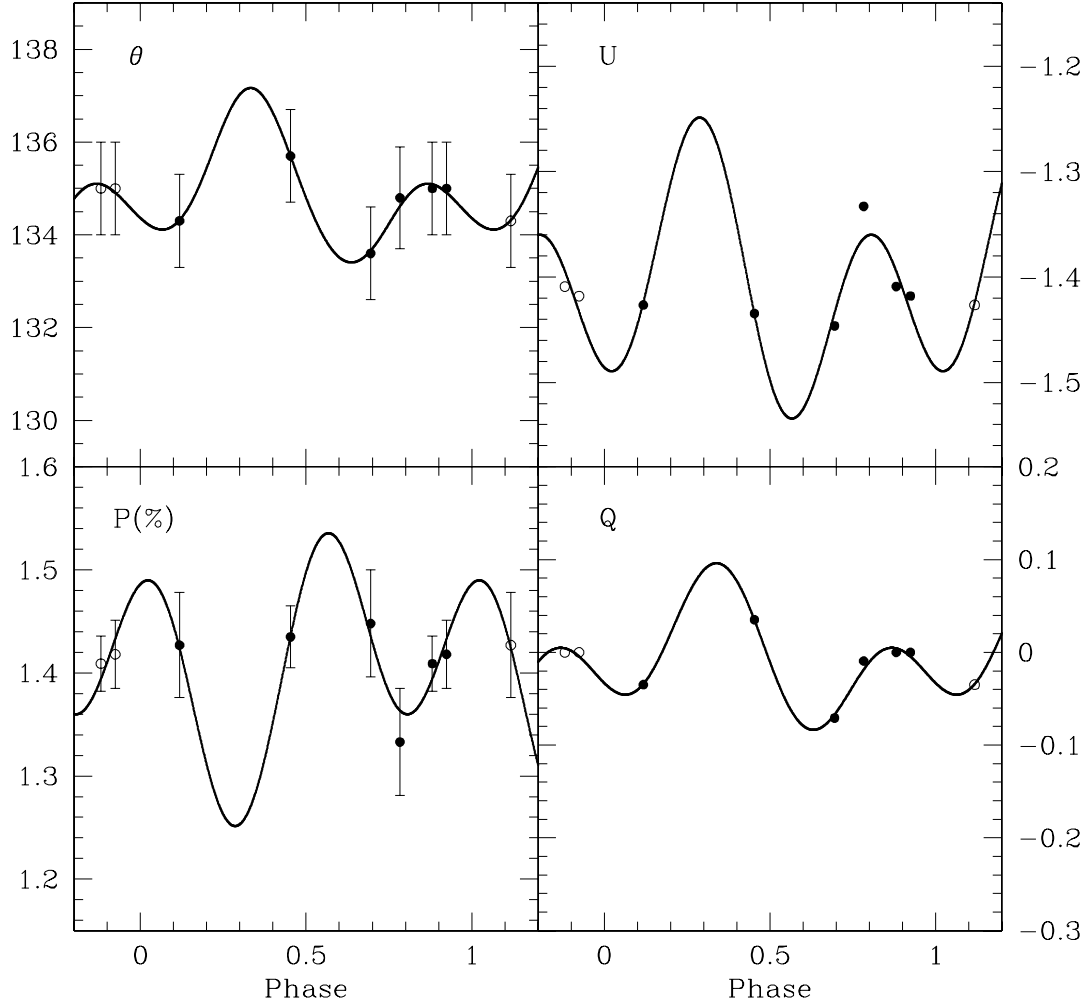


Fig. 11.— Subset of the polarimetric observations of NTT 160905-1859, obtained between 1998 May 13 and June 1.

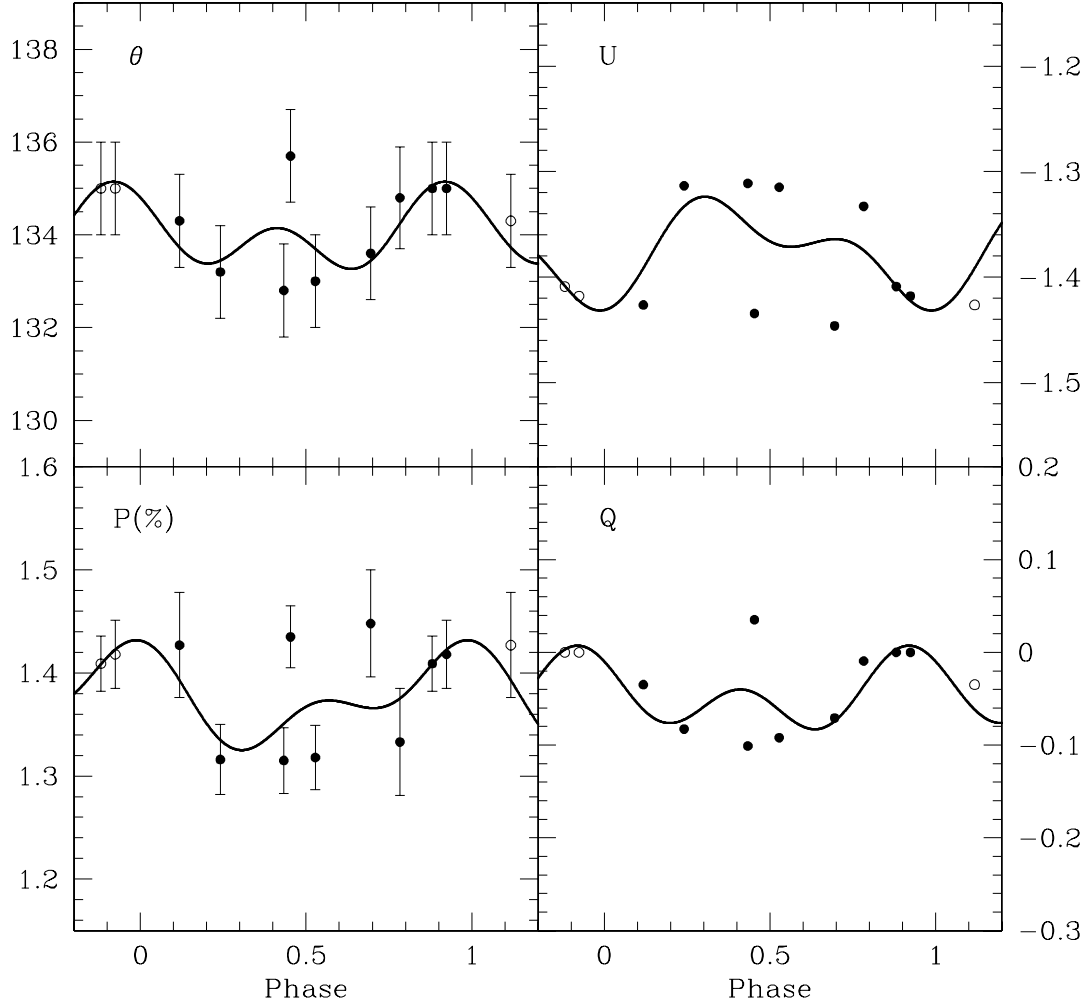


Fig. 12.— Subset of the polarimetric observations of NTT 160905-1859, obtained between 1998 April 27 and June 1, thus including the data presented in the preceding figure.

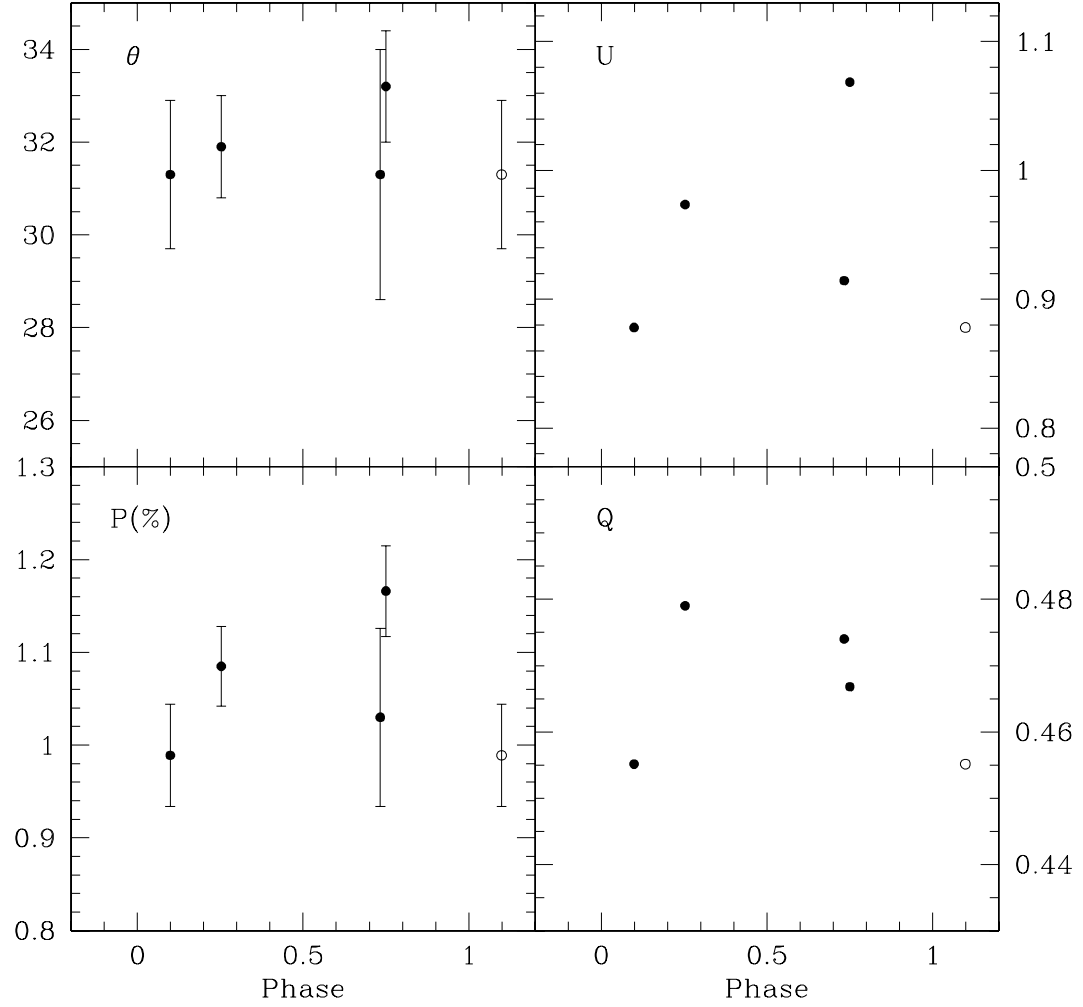


Fig. 13.— Polarimetric observations of Haro 1-14C. One atypical observation with a position angle different by  $100^\circ$  is not shown.

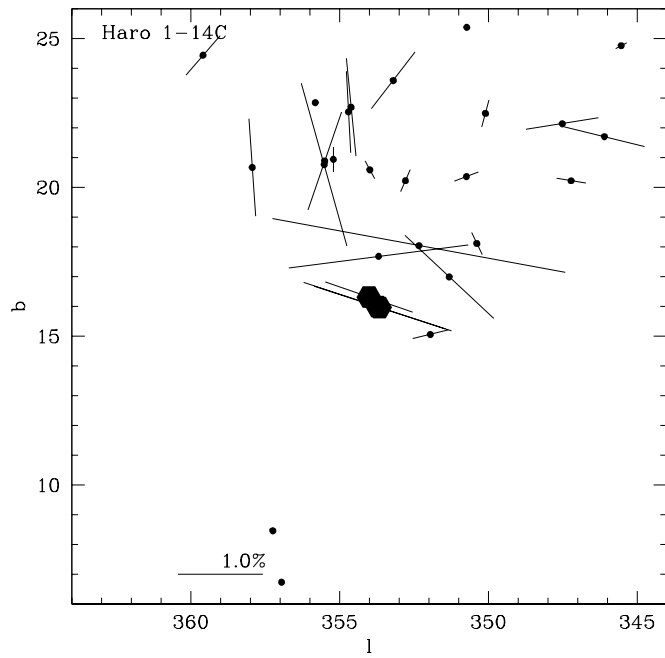


Fig. 14.— Map of the interstellar polarization in the vicinity of Haro 1-14C (at the center of the map), NTTs 162814-2427 and NTTs 162819-2423S (both below center, at  $\approx 0^\circ.5$  of Haro 1-14C). The stars selected to calculate the IS polarization are within 62 pc of those targets.

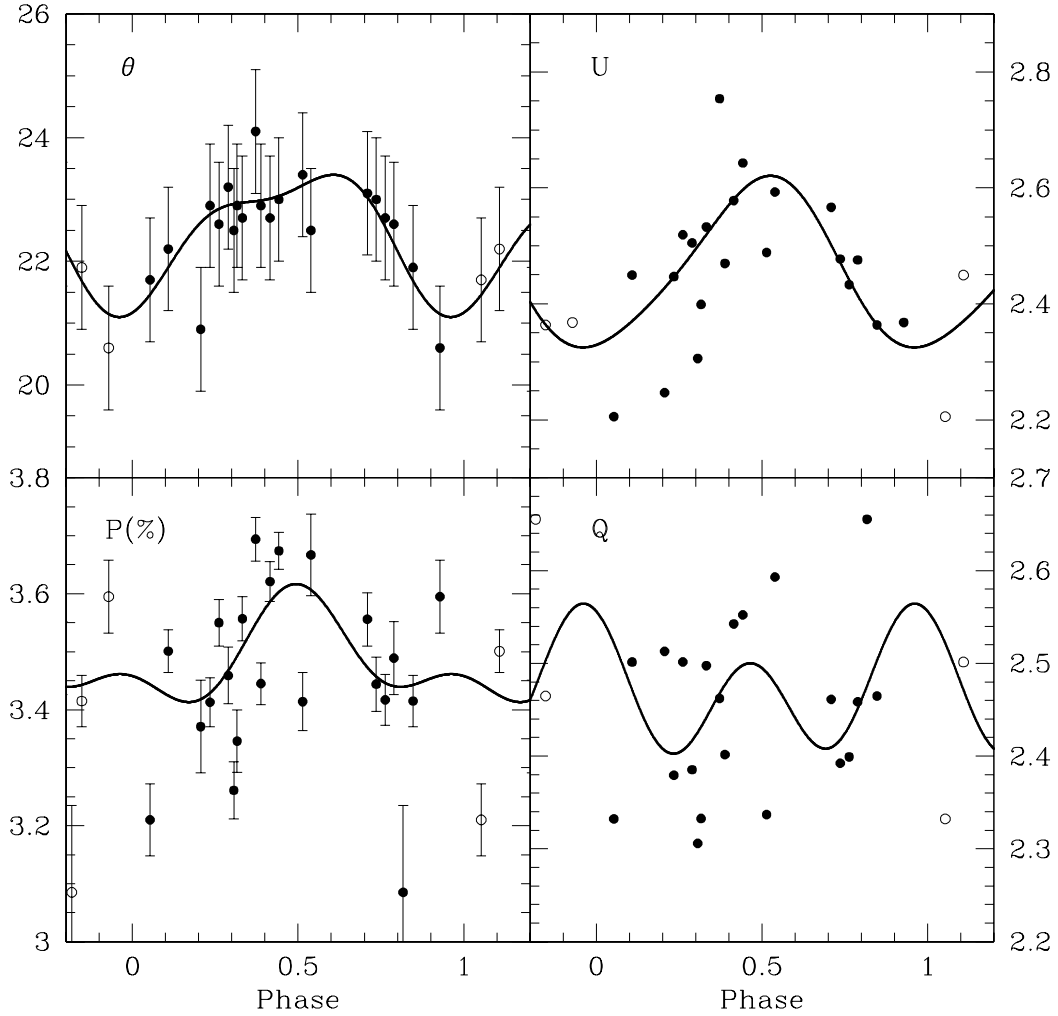


Fig. 15.— Polarimetric observations of NTTS 162814-2427. The star is clearly variable, but non-periodic variations introduce a lot of scatter in the possible periodic variations. One atypical point, taken in 1997 June, is not shown since its position angle and polarization are below the rest of the data.

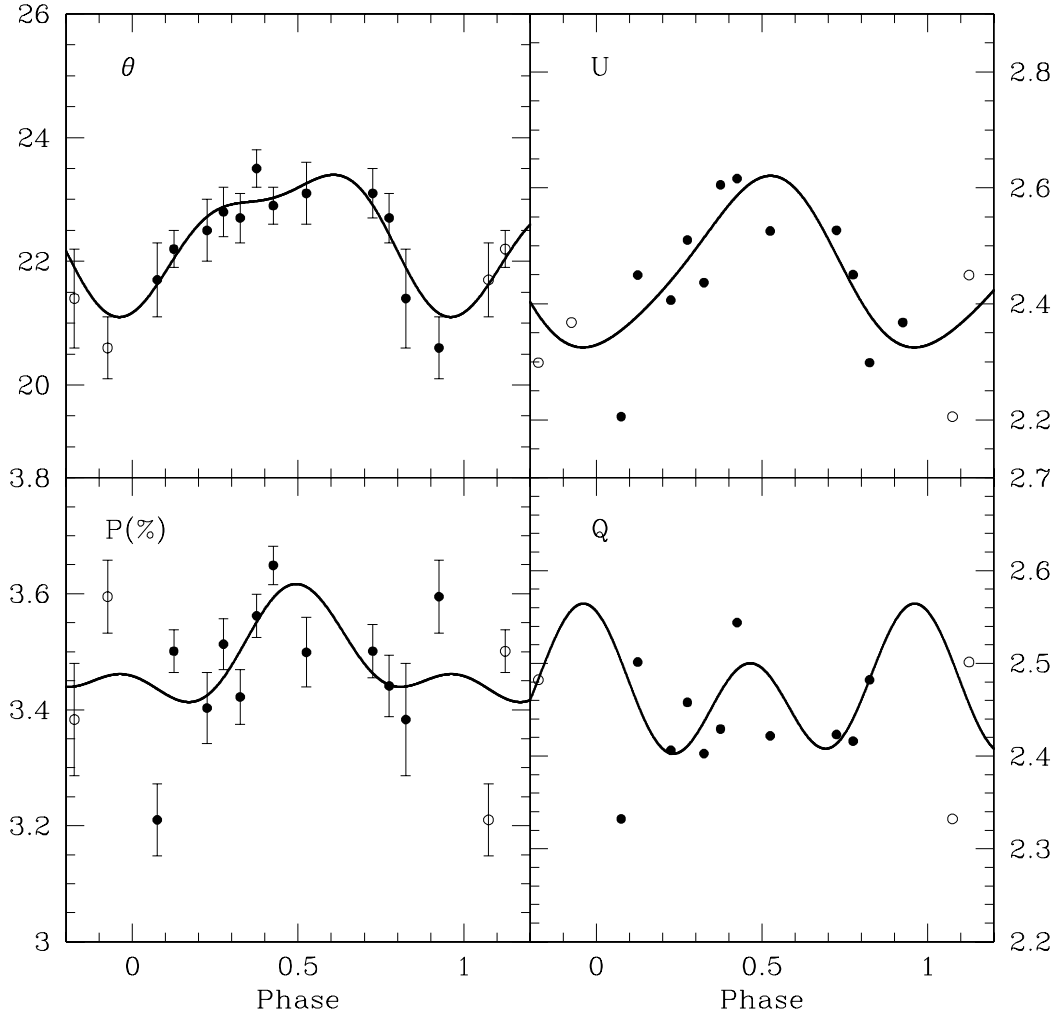


Fig. 16.— Binned data for the polarimetric observations of NTTS 162814-2427 that reveal clear single-periodic variations in position angle and the  $U$  parameter.

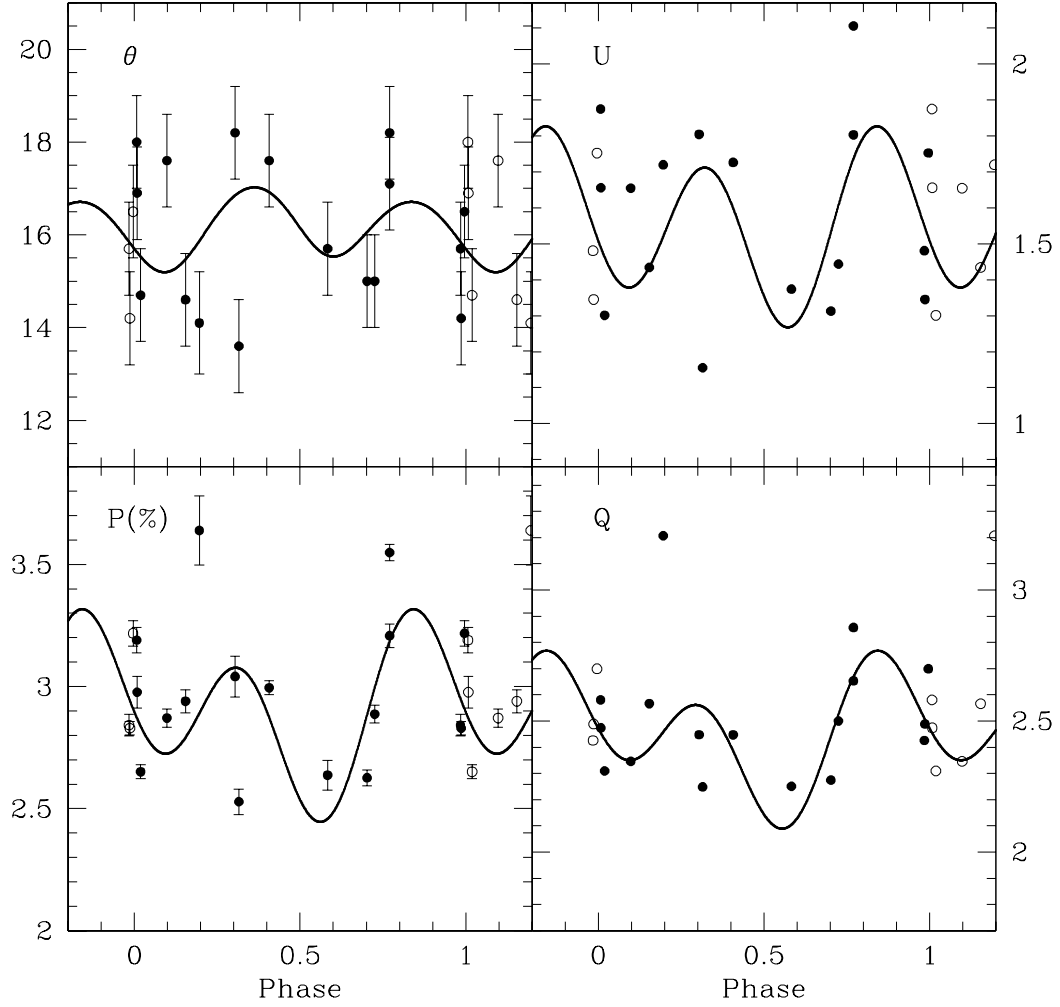


Fig. 17.— Polarimetric observations of NTTS 162819-2423S, the South binary of this quadruple system. This star is highly variable, but some of the variability can be attributed to measurement that included also the North component.

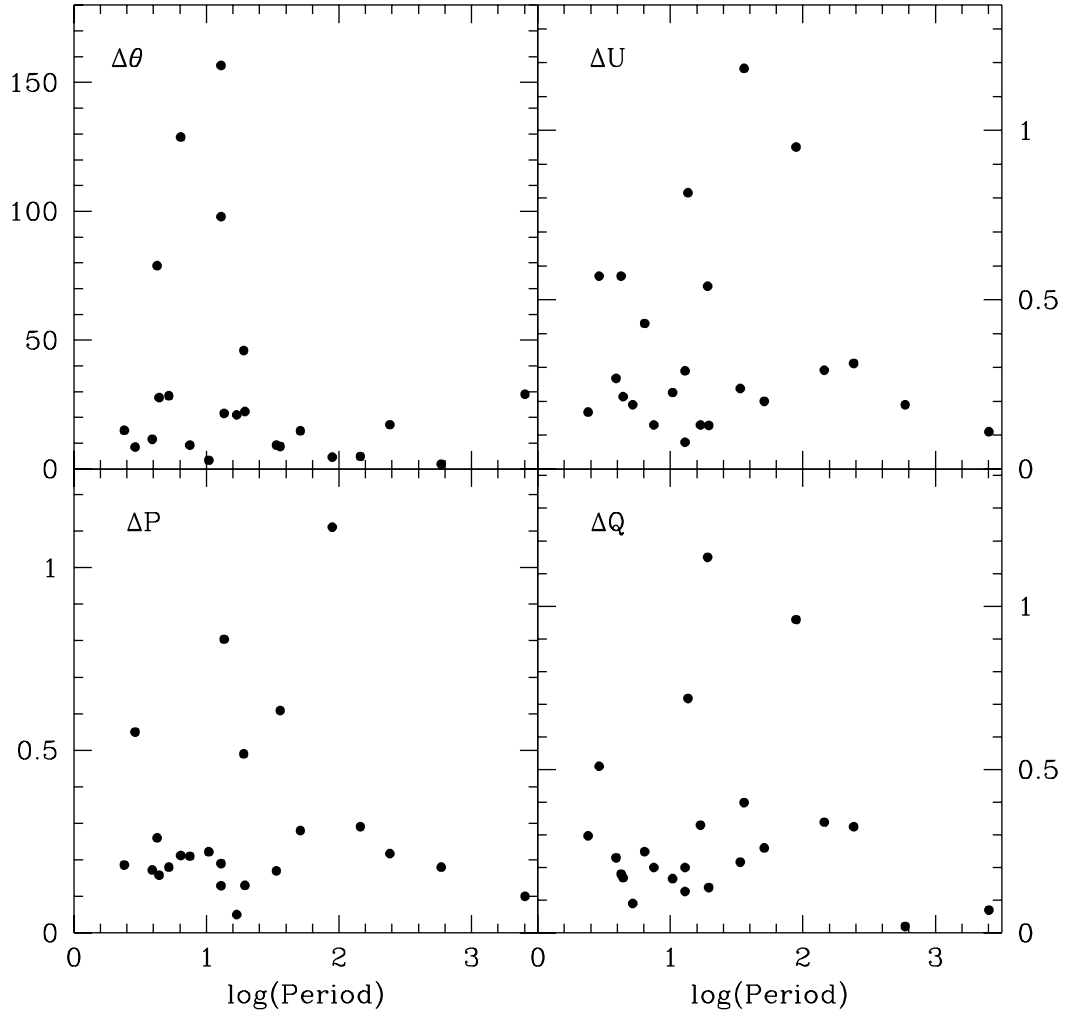


Fig. 18.— Amplitude of the polarimetric variations as a function of the orbital period.



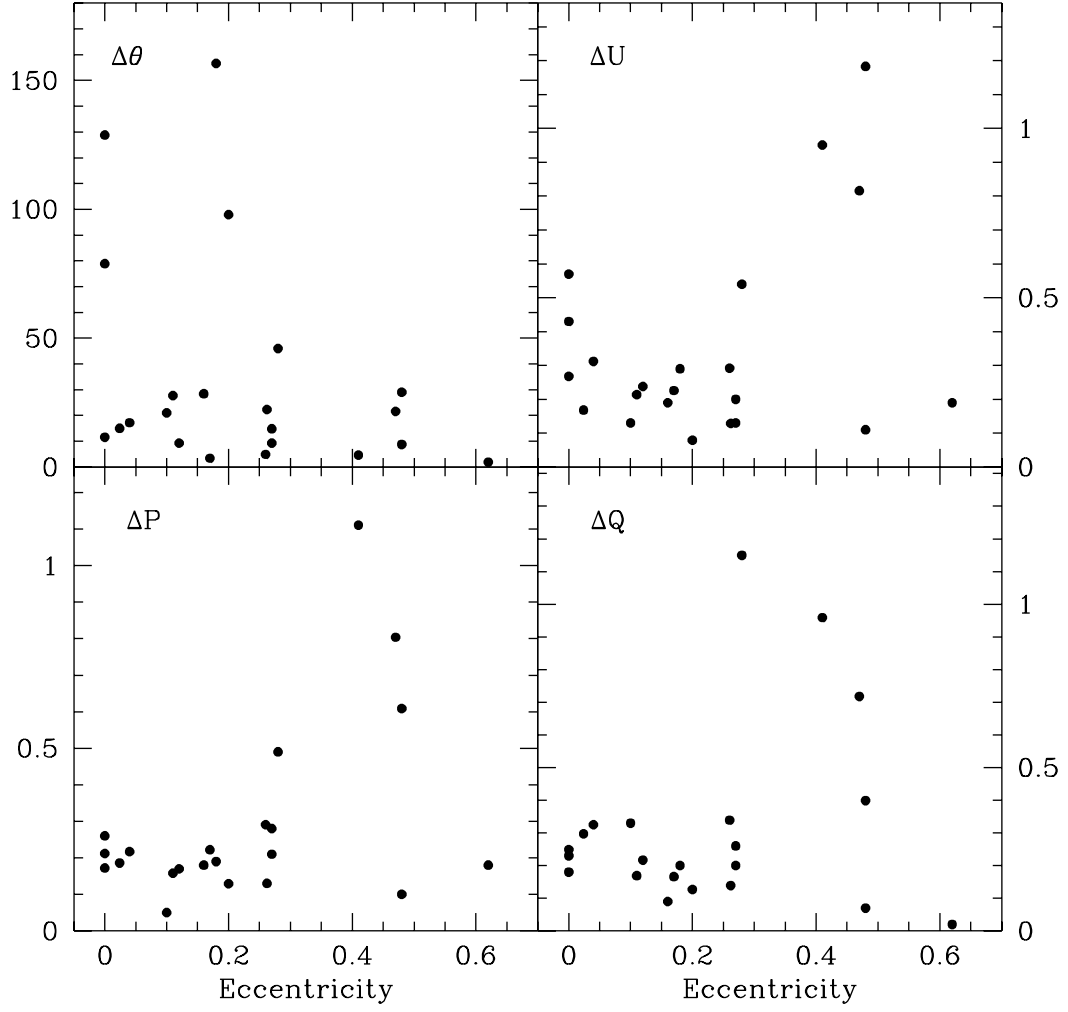


Fig. 19.— Amplitude of the polarimetric variations as a function of the orbital eccentricity.

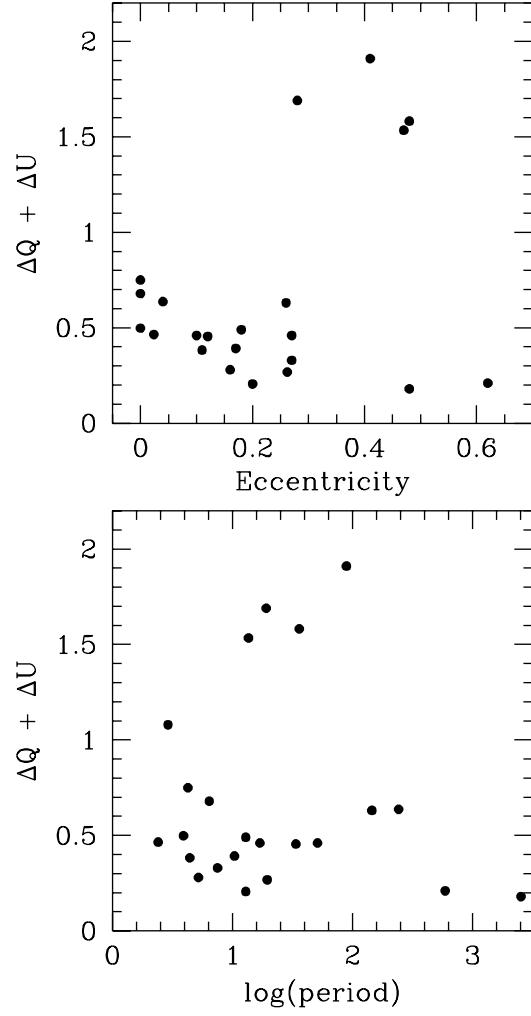


Fig. 20.— Sum of the variations seen in the Stokes parameters  $Q$  and  $U$  as a function of the orbital period and eccentricity.

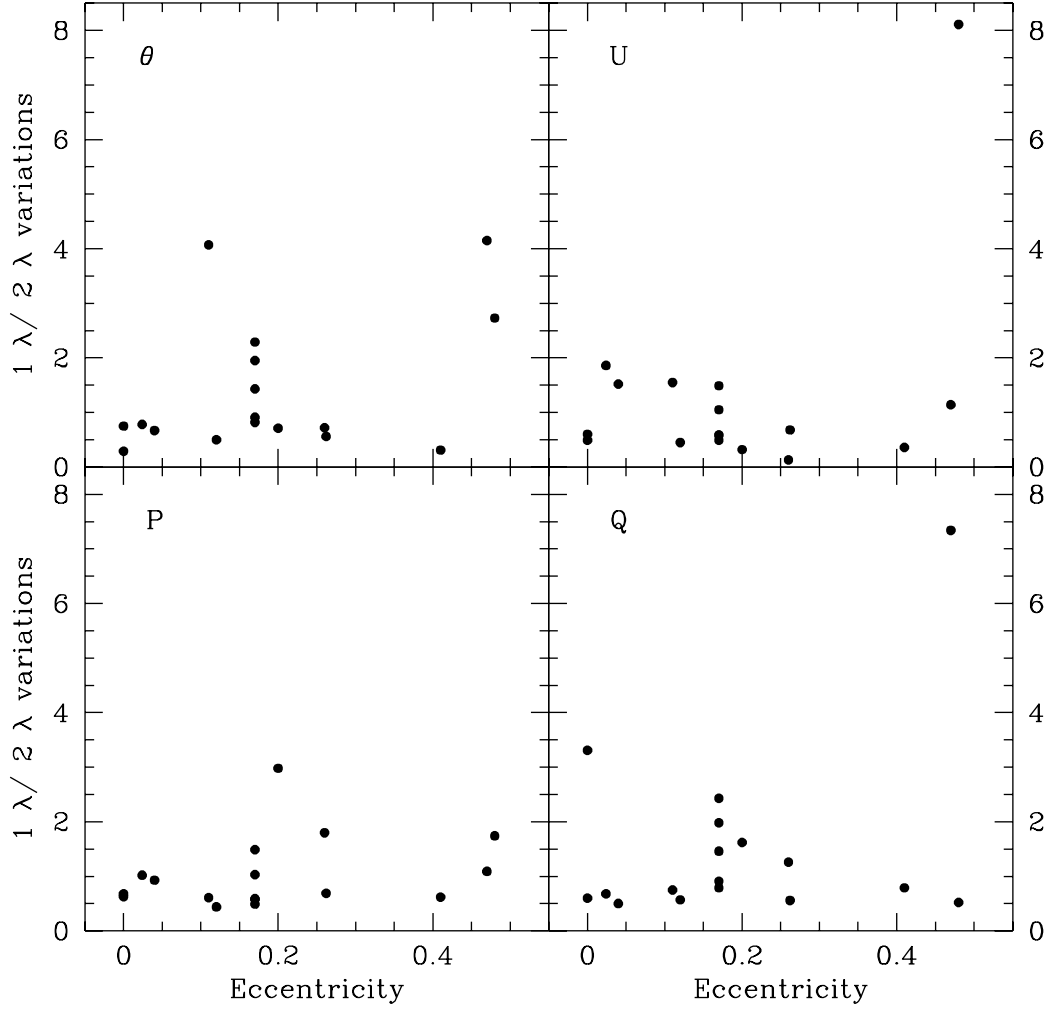


Fig. 21.— Ratio of the amplitude of the single-periodic variations over the amplitude of the double-periodic variations.

Table 1. Identification, coordinates, and location of the PMS binaries

Star	HBC <sup>1</sup>	Other Names	$\alpha^2$ (2000.0)	$\delta^2$ (2000.0)	Location
NTTS 155808-2219	...	ScoPMS 20	16 01 06	-22 27 00	Upper Sco
NTTS 155913-2233	...	ScoPMS 23	16 02 11	-22 41 28	Upper Sco
NTTS 160814-1857	630	ScoPMS 44, Wa OPH 1, V1000 Sco	16 11 09	-19 04 46	Upper Sco (B40)
NTTS 160905-1859	633	ScoPMS 48, Wa OPH 2, V1001 Sco	16 11 59	-19 06 53	Upper Sco (B40)
Haro 1-14C	644	...	16 31 05	-24 04 40	$\rho$ Oph B42
NTTS 162814-2427	...	ROX 42	16 31 16	-24 34 01	$\rho$ Oph B42
NTTS 162819-2423S	...	ROX 43A	16 31 20	-24 30 04	$\rho$ Oph B42

<sup>1</sup>HBC numbers come from the Herbig and Bell Catalog (Herbig & Bell 1988).

<sup>2</sup>All coordinates come from SIMBAD.

Table 2. Spectroscopic and orbital information for the PMS binaries

Star <sup>1</sup>	Spectral Type	Ref.	Type <sup>2</sup>	Ref.	sgl/ <sup>3</sup> dbl	Ref.	Period (d)	Ecc.	Ref.	Inc. (°)	Ref.	Dist. <sup>4</sup> (pc)	Ref.
NTTS 155808-2219 (3)	...	...	...	...	dbl	1	16.925	0.10	2	...	...	...	...
NTTS 155913-2233 (3)	K5 IV	3	WT	1	sgl	2	2.42378	0.024	1	...	...	160	...
NTTS 160814-1857 (2)	K2 IV + M2-M3	3	WT	4	sgl	1	144.7	0.26	2	...	...	150	4
NTTS 160905-1859 (2)	K0 IV + M3 IV	3	WT	4	sgl	1	10.400	0.17	2	...	...	150	4
Haro 1-14C (2)	K3	5	...	...	sgl	2	591	0.62	2	...	...	125	...
NTTS 162814-2427 (3)	K4-K5	6	WT	6	dbl	1	35.95	0.48	2	≈ 71	7	125	1
NTTS 162819-2423S (2)	G8	1	WT	1	sgl	1	89.1	0.41	2	~ 60	7	125	...

<sup>1</sup>The numbers in parenthesis after each object indicate the number of stars known in each system.

<sup>2</sup>Type of PMS star: WT (weak-line TTS)

<sup>3</sup>Single-line (sgl) or double-line (dbl) spectroscopic binary.

<sup>4</sup>When no reference is indicated, we have used the known distance to the cloud.

References. — (1) Mathieu, Walter, & Myers (1989); (2) Mathieu (1994) and references cited; (3) Walter et al. (1994); (4) Walter (1986); (5) Herbig & Bell (1988) (HBC catalog) and references cited; (6) Lee, Martín, & Mathieu (1994); (7) Jensen & Mathieu (1997)

Table 3. Average observed polarization, origin of the polarization, and estimate of the intrinsic polarization for the PMS binaries

Star	$P_{\text{ave}}^1$ (%)	$\theta_{\text{ave}}^1$ ( $^\circ$ )	$N_{\text{obs}}$	Origin of Polarization <sup>2</sup>	$P_{\text{IS}}^3$ (%)	$\sigma(P_{\text{IS}})$ (%)	$\theta_{\text{IS}}^3$ ( $^\circ$ )	$\sigma(\theta_{\text{IS}})$ ( $^\circ$ )	$N_{\text{IS}}$	Radius ( $^\circ$ )	Distance Interval ( $\pm$ pc)	$P_{\star}^4$ (%)	$\theta_{\star}^4$ ( $^\circ$ )
V773 Tau	0.35	88	6	IS + *	0.92	0.20	72	36	24	15	85	0.55	152
LkCa 3	0.05	76	12	IS + *	0.35	0.08	8	18	23	15	70	0.35	95
V826 Tau	0.85	67	11	* + IS	0.21	0.04	131	32	32	15	80	0.97	63
UZ Tau E/W	0.80	16	2	IS + *	0.68	0.16	17	14	26	15	70	0.2	13
DQ Tau	0.57	79	1	IS + *	0.35	0.09	85	17	19	12	80	0.28	72
NTTS 045251+3016	0.10	107	3	* + IS	0.10	0.03	58	9	18	15	80	0.14	126
GW Ori	0.61	126	11	* + IS	0.74	0.16	41	30	30	10	200	1.26	129
Par 1540	0.83	77	19	IS + *	1.37	0.25	64	5	28	1.0	235	0.59	135
Par 2486	0.14	63	6	IS + *	1.31	0.24	73	5	32	1.0	235	1.02	164
Ori 429	0.24	72	5	IS + *	1.01	0.23	92	6	21	2	235	0.72	8
Par 2494	0.16	46	29	IS + *	1.10	0.17	78	5	48	2	235	0.91	173
Ori 569	0.18	76	4	IS + *	0.88	0.12	90	5	68	6	235	0.62	4
W 134	0.22	32	11	IS + *	0.26	0.05	177	4	20	8	350	0.26	60
VSB 126	0.16	66	6	* + IS	0.26	0.05	177	4	20	8	350	0.36	79
NTTS 155808-2219	0.48	139	4	* + IS	0.34	0.07	88	24	22	6	80	0.62	153
NTTS 155913-2233	0.49	124	36	* + IS	0.23	0.05	73	26	22	6	80	0.57	134
NTTS 155913-2233 <sup>5</sup>	0.53	127	6	* + IS	0.23	0.05	73	26	22	6	80	0.64	137
NTTS 160814-1857	1.94	117	9	IS + *	1.51	0.26	123	10	24	8	75	0.70	105
NTTS 160905-1859	1.38	134	34	IS + *	1.16	0.20	123	10	24	8	75	0.58	155
NTTS 160905-1859 <sup>5</sup>	1.09	134	4	IS + *	1.16	0.20	123	10	24	8	75	0.43	178
Haro 1-14C	1.08	34	5	IS + *	1.08	0.21	24	18	20	10	62	0.37	64
NTTS 162814-2427	3.50	22	22	* + IS	1.62	0.32	25	16	19	10	62	2.09	20
NTTS 162819-2423S	2.92	16	17	IS + *	1.83	0.36	25	16	19	10	62	1.47	6

<sup>1</sup>Weighted averages of the observed  $P$  and  $\theta$ . The averages do not include atypical observations.

<sup>2</sup>Probable origin of the polarization. A \* symbol indicates intrinsic polarization; IS stands for interstellar polarization. If IS comes before a \* symbol, the IS component of the polarization is probably stronger than the intrinsic one.

<sup>3</sup>Estimate of the IS polarization at the location of the PMS binary based on data from the Heiles (2000) catalog. See text for details.

<sup>4</sup>Intrinsic polarization obtained after subtracting the estimated IS polarization.

<sup>5</sup>The additional entries for NTTS 155913-2233 and NTTS 160905-1859 come from the Pic-du-Midi data taken in the  $V$  filter.

Table 4. Amplitude of the polarimetric variations <sup>1</sup>

Star	Wavelength (Å)	$\Delta P$ (%)	$\Delta\theta$ (°)	$\Delta Q$ (%)	$\Delta U$ (%)	$N_{\text{obs}}$
V773 Tau	7660	0.28	15	0.26	0.20	6
LkCa 3	7660	0.13	98	0.13	0.08	12
V826 Tau	7660	0.17	12	0.23	0.27	11
UZ Tau E/W	7660	0.49	46	1.15	0.54	2
NTTS 045251+3016	7660	0.10	29	0.07	0.11	3
GW Ori	7660	0.22	17	0.33	0.31	11
Par 1540	7660	0.17	9	0.22	0.24	19
Par 2486	7660	0.18	28	0.09	0.19	6
Ori 429	7660	0.21	9	0.20	0.13	5
Par 2494	7660	0.13	22	0.14	0.13	29
Ori 569	7660	0.26	79	0.18	0.57	4
W 134	7660	0.21	129	0.25	0.43	11
VSB 126	7660	0.19	157	0.20	0.29	6
NTTS 155808-2219	7660	0.05	21	0.33	0.13	4
NTTS 155913-2233	7660	0.19	15	0.30	0.17	36
...	5550	0.21	7	0.15	0.19	6
NTTS 160814-1857	7660	0.29	5	0.34	0.29	9
NTTS 160905-1859	7660	0.22	3	0.17	0.23	34
...	5550	0.09	4	0.16	0.09	4
Haro 1-14C	7660	0.18	2	0.02	0.19	4
NTTS 162814-2427	7660	0.61	9	0.40	1.18	22
NTTS 162819-2423S	7660	1.11	5	0.96	0.95	17
AK Sco <sup>2</sup>	5250	0.80	22	0.72	0.82	27
EK Cep <sup>2</sup>	5500	0.16	28	0.17	0.21	36
MWC 1080 <sup>3</sup>	7660	0.55	9	0.51	0.57	62

<sup>1</sup>Difference between the minimum and maximum values of the polarization, excluding, in some cases, atypical observations. The values  $\Delta Q$  and  $\Delta U$  are not calculated from  $\Delta P$  and  $\Delta\theta$ , but from the maximum and minimum values of  $Q$  and  $U$ .

<sup>2</sup>Data for AK Sco and EK Cep will be presented in future papers.

<sup>3</sup>Data for MWC 1080 were presented in Paper III.

Table 5. Results of the variability tests at 7660Å and 5550Å

Star	Wavelength (Å)	$N_{\text{obs}}$		$\sigma_{\text{sample}}$	$\sigma_{\text{mean}}$	$Z \pm \sigma_Z$	$P\chi^2$ 1 $\sigma$	$P\chi^2$ 1.5 $\sigma$
NTTS 155808-2219	7660	4	$Q$	0.1531	0.0350	2.35 0.41	1.00	0.94
			$U$	0.0539	0.0350	0.76 0.41	0.34	0.13
NTTS 155913-2233	7660	36	$Q$	0.0597	0.0059	1.42 0.12	1.00	0.35
			$U$	0.0433	0.0059	1.09 0.12	0.78	0.01
	5550	6	$Q$	0.0604	0.0255	0.95 0.32	0.10	0.03
			$U$	0.0697	0.0255	1.00 0.32	0.11	0.03
NTTS 160814-1857	7660	9	$Q$	0.0956	0.0165	1.52 0.25	0.98	0.59
			$U$	0.1040	0.0165	2.37 0.25	1.00	0.99
NTTS 160905-1859	7660	34	$Q$	0.0478	0.0070	1.15 0.12	0.89	0.03
			$U$	0.0520	0.0070	1.32 0.12	0.99	0.18
	5550	4	$Q$	0.0867	0.0409	1.09 0.41	0.19	0.09
			$U$	0.0423	0.0409	0.49 0.41	0.04	0.01
Haro 1-14C	7660	4	$Q$	0.0104	0.0268	0.21 0.41	0.01	0.00
			$U$	0.0831	0.0268	1.58 0.41	0.93	0.64
NTTS 162814-2427	7660	22	$Q$	0.1055	0.0097	1.91 0.15	1.00	0.96
			$U$	0.2287	0.0097	3.34 0.15	1.00	1.00
NTTS 162819-2423S	7660	17	$Q$	0.2430	0.0099	4.55 0.18	1.00	1.00
			$U$	0.2527	0.0099	6.52 0.18	1.00	1.00



Table 6. Classification of the observed PMS binaries, according to their variability at 7660Å

Variability Classification	PMS Binary
Variable	NTTS 160814-1857 (9), NTTS 162819-2423S (17), NTTS 162814-2427 <sup>1</sup> (22)
Suspected variable	NTTS 155808-2219 (4), NTTS 155913-2233 <sup>1</sup> (36) NTTS 160905-1859 <sup>1</sup> (34), Haro 1-14C (4)
Possibly constant	...
Constant	...

<sup>1</sup>These stars were sometimes observed to have very different polarization and/or position angle values (well above or below the majority of the data points) so their variability is based on data excluding those atypical values.

Note. — The number of observations used for the variability tests is indicated in parentheses.

Table 7. Polarization data for NTTS 155808-2219 at 7660Å

UT Date	JD 2400000.0+	Phase <sup>1</sup>	P (%)	$\sigma(P)$ (%)	$\theta$ (°)	$\sigma(\theta)$ (°)
1997 Apr 12	50550.849	0.454	0.481	0.063	152.7	3.8
1997 Apr 16	50554.827	0.689	0.474	0.064	132.2	3.8
1997 Jun 7	50606.708	0.755	0.522	0.102	133.5	5.6
1998 May 1	50934.813	0.141	0.479	0.067	134.8	4.0

<sup>1</sup>Calculated with the ephemeris  $2449900.0 + 16.925E$  (Mathieu 1994).

Table 8. Polarization data for NTTS 155913-2233 at 7660Å

UT Date	JD 2400000.0+	Phase <sup>1</sup>	P (%)	$\sigma(P)$ (%)	$\theta$ (°)	$\sigma(\theta)$ (°)
1995 May 2	49839.724	0.518	0.472	0.025	123.2	1.5
1995 May 4	49841.771	0.362	0.456	0.037	122.4	2.3
1995 May 7	49844.782	0.605	0.220	0.073	161.7	9.4
1995 May 9	49846.667	0.382	0.579	0.037	122.1	1.8
1995 May 10	49847.683	0.802	0.495	0.022	122.2	1.2
1995 Aug 28	49957.543	0.128	0.500	0.040	120.3	2.3
1995 Aug 31	49960.532	0.361	0.575	0.052	116.9	2.6
1995 Sep 3	49963.531	0.598	0.424	0.066	123.1	4.5
1996 Apr 19	50192.802	0.190	0.491	0.053	129.4	3.1
1996 Apr 28	50201.789	0.898	0.443	0.030	126.9	1.9
1996 Apr 29	50202.804	0.317	0.556	0.034	120.7	1.7
1996 May 3	50206.780	0.957	0.482	0.040	123.4	2.4
1996 May 7	50210.743	0.593	0.470	0.027	127.3	1.6
1996 Jun 2	50236.698	0.301	0.467	0.069	123.9	4.3
1996 Jul 7	50271.600	0.701	0.509	0.027	122.0	1.5
1997 Feb 11	50490.909	0.183	0.486	0.028	125.0	1.6
1997 Apr 2	50540.832	0.780	0.504	0.052	126.6	3.0
1997 Apr 3	50541.811	0.184	0.471	0.033	121.3	2.0
1997 Apr 5	50543.839	0.021	0.480	0.031	123.0	1.9
1997 Apr 10	50548.786	0.062	0.461	0.029	129.1	1.8
1997 Apr 11	50549.766	0.466	0.462	0.028	125.4	1.7
1997 Apr 11	50549.872	0.510	0.476	0.046	168.2	2.8
1997 Apr 12	50550.781	0.885	0.471	0.028	125.3	1.7
1997 Apr 15	50553.786	0.125	0.472	0.027	121.5	1.6
1997 Apr 16	50554.784	0.536	0.570	0.033	126.7	1.7
1997 Jun 3	50602.627	0.276	0.474	0.045	123.9	2.7
1997 Jun 4	50603.728	0.730	0.452	0.044	123.3	2.8
1997 Jun 5	50604.678	0.122	0.429	0.034	127.3	2.3
1997 Jun 6	50605.609	0.506	0.399	0.062	127.6	4.5
1997 Jun 6	50605.725	0.554	0.584	0.074	120.8	3.6
1997 Jun 7	50606.602	0.915	0.430	0.043	123.4	2.9
1997 Jun 7	50606.738	0.972	0.420	0.052	126.2	3.5

Table 8—Continued

UT Date	JD 2400000.0+	Phase <sup>1</sup>	P (%)	$\sigma(P)$ (%)	$\theta$ (°)	$\sigma(\theta)$ (°)
1997 Jun 9	50608.608	0.743	0.528	0.034	124.1	1.8
1997 Jun 9	50608.741	0.798	0.536	0.043	127.4	2.3
1997 Jun 15	50614.731	0.269	0.398	0.070	131.9	5.0
1998 Apr 29	50932.838	0.514	0.420	0.054	127.4	3.7
1998 May 1	50934.781	0.315	0.448	0.036	118.8	2.3
1999 June 11	51340.609	0.751	0.567	0.034	124.6	1.7

<sup>1</sup>Calculated with the ephemeris  $2445999.2 + 2.42378E$  (Mathieu et al. 1989).

Table 9. Polarization data for NTTS 155913-2233 at 5550Å

UT Date	JD 2400000.0+	Phase <sup>1</sup>	P (%)	$\sigma(P)$ (%)	$\theta$ (°)	$\sigma(\theta)$ (°)
1994 May 6	49479.557	0.924	0.518	0.048	128.4	2.3
1994 May 8	49481.555	0.745	0.495	0.080	129.6	4.0
1994 May 9	49482.517	0.142	0.598	0.059	123.1	2.5
1994 May 10	49483.513	0.553	0.653	0.077	126.2	2.9
1994 May 11	49484.524	0.970	0.447	0.064	129.0	3.6
1994 May 12	49485.516	0.379	0.471	0.063	125.1	3.3

<sup>1</sup>Calculated with the ephemeris  $2445999.2 + 2.42378E$  (Mathieu et al. 1989).

Table 10. Polarization data for NTTS 160814-1857 at 7660Å and 5550Å

UT Date	JD 2400000.0+	Phase <sup>1</sup>	P (%)	$\sigma(P)$ (%)	$\theta$ (°)	$\sigma(\theta)$ (°)
1994 May 6 <sup>2</sup>	49479.531	0.818	1.613	0.130	118.3	2.0
1995 May 9	49846.763	0.356	1.926	0.065	115.0	1.0
1996 May 8	50211.700	0.878	1.788	0.064	119.9	1.0
1997 Apr 11	50549.737	0.214	1.909	0.048	116.3	1.0
1997 Apr 12	50550.715	0.221	1.934	0.052	118.4	1.0
1997 Jun 5	50604.730	0.594	2.026	0.054	117.6	1.0
1998 Apr 29	50932.660	0.860	1.817	0.035	116.0	1.0
1999 May 22	51320.633	0.542	2.045	0.035	118.6	1.0
1999 Jun 11	51340.733	0.680	2.079	0.076	118.0	1.0
1999 Jun 12	51341.729	0.687	1.953	0.063	116.7	1.0

<sup>1</sup>Calculated with the ephemeris  $2446003 + 144.7E$  (Mathieu et al. 1989).

<sup>2</sup>Data obtained at 5550Å.

Table 11. Polarization data for NTTS 160905-1859 at 7660Å

UT Date	JD 2400000.0+	Phase <sup>1</sup>	P (%)	$\sigma(P)$ (%)	$\theta$ (°)	$\sigma(\theta)$ (°)
1995 May 9	49846.729	0.012	1.332	0.064	135.4	1.4
1996 May 3	50206.816	0.636	1.264	0.087	140.7	2.0
1996 May 7	50210.780	0.017	1.320	0.036	135.2	1.0
1996 Jun 2	50236.624	0.502	1.430	0.091	134.9	1.8
1997 Apr 2	50540.794	0.749	1.355	0.044	135.3	1.0
1997 Apr 3	50541.765	0.842	1.346	0.035	132.9	1.0
1997 Apr 5	50543.865	0.044	1.408	0.046	135.5	1.0
1997 Apr 10	50548.821	0.521	1.264	0.039	132.5	1.0
1997 Apr 11	50549.800	0.615	1.370	0.034	133.8	1.0
1997 Apr 12	50550.744	0.706	1.428	0.034	134.5	1.0
1997 Apr 15	50553.746	0.994	1.373	0.035	134.2	1.0
1997 Apr 16	50554.747	0.091	1.428	0.040	133.8	1.0
1997 Jun 3	50602.732	0.705	1.427	0.083	135.4	1.7
1997 Jun 4	50603.616	0.790	1.389	0.053	135.2	1.1
1997 Jun 5	50604.595	0.884	1.395	0.050	132.3	1.0
1997 Jun 6	50605.693	0.989	1.307	0.055	135.5	1.2
1997 Jun 7	50606.678	0.084	1.332	0.045	133.7	1.0
1997 Jun 9	50608.675	0.276	1.486	0.035	134.2	1.0
1997 Jun 15	50614.687	0.854	1.370	0.043	134.4	1.0
1997 Jul 7	50636.626	0.964	1.353	0.048	134.4	1.0
1997 Jul 11	50640.605	0.346	1.443	0.041	134.8	1.0
1997 Sep 9	50700.541	0.109	1.426	0.065	132.4	1.3
1998 Apr 27	50930.708	0.241	1.316	0.034	133.2	1.0
1998 Apr 29	50932.713	0.433	1.315	0.032	132.8	1.0
1998 Apr 30	50933.701	0.528	1.318	0.031	133.0	1.0
1998 May 1	50934.670	0.622	1.419	0.036	120.7	1.0
1998 May 13	50946.745	0.783	1.333	0.052	134.8	1.1
1998 May 14	50947.768	0.881	1.409	0.027	135.0	1.0
1998 May 20	50953.720	0.453	1.435	0.030	135.7	1.0
1998 May 25	50958.613	0.924	1.418	0.033	135.0	1.0
1998 May 27	50960.627	0.118	1.427	0.051	134.3	1.0
1998 Jun 1	50966.634	0.695	1.448	0.052	133.6	1.0

Table 11—Continued

UT Date	JD 2400000.0+	Phase <sup>1</sup>	P (%)	$\sigma(P)$ (%)	$\theta$ (°)	$\sigma(\theta)$ (°)
1999 May 22	51320.698	0.740	1.417	0.043	135.5	1.0
1999 Jun 12	51341.610	0.750	1.400	0.048	134.7	1.0
1999 Jun 13	51342.611	0.847	1.413	0.050	133.9	1.0
1999 Jun 14	51343.601	0.942	1.411	0.055	133.5	1.1

<sup>1</sup>Calculated with the ephemeris  $2445998.6 + 10.40E$  (Mathieu et al. 1989).



Table 12. Polarization data for NTTS 160905-1859 at 5550Å

UT Date	JD 2400000.0+	Phase <sup>1</sup>	P (%)	$\sigma(P)$ (%)	$\theta$ (°)	$\sigma(\theta)$ (°)
1994 May 6	49479.510	0.702	1.059	0.087	132.6	2.0
1994 May 8	49481.597	0.903	1.068	0.105	136.3	2.5
1994 May 9	49482.549	0.995	1.082	0.0065	132.0	1.5
1994 May 11	49484.583	0.190	1.150	0.0085	136.2	2.0

<sup>1</sup>Calculated with the ephemeris  $2445998.6 + 10.40E$  (Mathieu et al. 1989).

Table 13. Polarization data for Haro 1-14C at 7660Å

UT Date	JD 2400000.0+	Phase <sup>1</sup>	P (%)	$\sigma(P)$ (%)	$\theta$ (°)	$\sigma(\theta)$ (°)
1997 Apr 11	50549.860	0.099	0.989	0.055	31.3	1.6
1997 Jun 5	50604.749	0.192	1.074	0.199	133.2	5.3
1997 Jun 6	45605.750	0.733	1.030	0.096	31.3	2.7
1997 Jul 11	50640.637	0.253	1.085	0.043	31.9	1.1
1998 May 1	50934.760	0.750	1.166	0.049	33.2	1.2

<sup>1</sup>Calculated with the ephemeris  $49900.0 + 591.0E$  (period from Mathieu 1994).

Table 14. Polarization data for NTTS 162814-2427 at 7660Å

UT Date	JD 2400000.0+	Phase <sup>1</sup>	P (%)	$\sigma(P)$ (%)	$\theta$ (°)	$\sigma(\theta)$ (°)
1995 May 10	49847.723	0.206	3.371	0.080	20.9	1.0
1996 May 7	50210.808	0.306	3.261	0.049	22.5	1.0
1996 Jul 9	50273.616	0.053	3.210	0.062	21.7	1.0
1997 Apr 3	50541.841	0.514	3.414	0.050	23.4	1.0
1997 Apr 10	50548.845	0.709	3.556	0.046	23.1	1.0
1997 Apr 11	50549.828	0.736	3.444	0.047	23.0	1.0
1997 Apr 12	50550.813	0.763	3.417	0.044	22.7	1.0
1997 Apr 15	50553.824	0.847	3.415	0.044	21.9	1.0
1997 Jun 3	50602.677	0.206	2.626	0.033	15.0	1.0
1997 Jun 4	50603.679	0.234	3.413	0.042	22.9	1.0
1997 Jun 5	50604.635	0.261	3.550	0.040	22.6	1.0
1997 Jun 6	50605.650	0.289	3.459	0.049	23.2	1.0
1997 Jun 7	50606.638	0.316	3.346	0.054	22.9	1.0
1997 Jun 9	50608.640	0.372	3.694	0.038	24.1	1.0
1997 Jun 15	50614.629	0.539	3.667	0.070	22.5	1.0
1997 Sep 9	50700.523	0.928	3.595	0.063	20.6	1.0
1998 Apr 27	50930.754	0.332	3.557	0.038	22.7	1.0
1998 Apr 29	50932.753	0.388	3.445	0.036	22.9	1.0
1998 Apr 30	50933.748	0.415	3.621	0.034	22.7	1.0
1998 May 1	50934.721	0.442	3.674	0.032	23.0	1.0
1998 May 25	50958.643	0.108	3.501	0.037	22.2	1.0
1999 Jun 13	51342.650	0.789	3.489	0.063	22.6	1.0
1999 Jun 14	51343.632	0.817	3.085	0.150	15.3	1.4

<sup>1</sup>Calculated with the ephemeris  $2445023.0 + 35.95E$  (Mathieu et al. 1989).

Table 15. Polarization data for NTTS 162819-2423S at 7660Å

UT Date	JD 2400000.0+	Phase <sup>1</sup>	P (%)	$\sigma(P)$ (%)	$\theta$ (°)	$\sigma(\theta)$ (°)
1995 May 7	49844.838	0.196	3.639	0.141	14.1	1.1
1996 May 7	50210.828	0.304	3.041	0.083	18.2	1.0
1996 May 8	50211.768	0.315	2.528	0.052	13.6	1.0
1996 Jun 1	50235.667	0.583	2.637	0.061	15.7	1.0
1996 Jul 7	50271.619	0.986	2.829	0.028	14.2	1.0
1997 Apr 3	50541.865	0.019	2.651	0.029	14.7	1.0
1997 Apr 10	50548.868	0.098	2.871	0.037	17.6	1.0
1997 Apr 15	50553.865	0.154	2.940	0.047	14.6	1.0
1997 Jun 3	50602.677	0.702	2.626	0.033	15.0	1.0
1997 Jun 5	50604.706	0.725	2.887	0.036	15.0	1.0
1997 Jun 9	50608.708	0.770	3.549	0.034	18.2	1.0
1997 Jun 9	50608.714	0.770	3.208	0.048	17.1	1.0
1998 Apr 29	50932.808	0.407	2.995	0.029	17.6	1.0
1999 Jun 11	51340.651	0.984	2.842	0.044	15.7	1.0
1999 Jun 12	51341.683	0.996	3.218	0.052	16.5	1.0
1999 Jun 13	51342.695	0.007	3.190	0.053	18.0	1.0
1999 Jun 13	51342.736	0.008	2.977	0.065	16.9	1.0

<sup>1</sup>Calculated with the ephemeris 2445996.0+89.1*E* (Mathieu et al. 1989).

Table 16. Noise analysis and orbital inclination from the BME model for some observed binaries

Star	$DQ$	$\gamma$	Noise <sup>1</sup> for $Q$	Noise for $U$	$i(\mathcal{O}2)$ ( $^\circ$ )	$\sigma(i(\mathcal{O}2))$ ( $^\circ$ )	$i(\mathcal{O}1)$ ( $^\circ$ )	$\sigma(i(\mathcal{O}1))$ ( $^\circ$ )
NTTS 155913-2233	0.202	12.2	0.16	0.22	96.7	8.8	23.4	84.5
..... set 1	0.276	6.6	0.23	0.24	95.5	9.7	87.8	17.3
..... set 2	0.248	8.1	0.20	0.23	103.0	19.4	88.6	18.7
NTTS 160814-1857	0.941	45.8	0.23	0.23	97.1	0.3	93.4	0.6
NTTS 160905-1859	0.281	6.3	0.29	0.24	84.4	8.1	150.2	68.8
..... set 1	0.106	44.6	0.34	0.13	95.6	7.7	100.0	15.8
..... set 2	0.190	13.9	0.34	0.15	93.2	14.4	66.8	37.4
..... set 3	0.143	24.3	0.10	0.31	98.4	17.1	99.4	40.7
..... set 4	0.256	7.6	0.44	0.51	112.2	35.0	86.6	25.1
NTTS 162814-2427 <sup>2</sup>	0.099	51.1	0.22	0.10	...	...	93.8	2.6

<sup>1</sup>The noise is the square root of the variance of the fit over the amplitude of the variations; the amplitude comes from the maximum values of the data and not from the fit.

<sup>2</sup>Since NTTS 162814-2427's eccentricity is above 0.3, only the BME results obtained from the first order make sense (Paper I).

Table 17. Other parameters returned by the BME model:  $\Omega$ , the orientation of the orbital plane, and moments of the distribution of the scatterers.

Star	$\Omega$ ( $^\circ$ )	$\sigma(\Omega)$ ( $^\circ$ )	$\tau_0 G$ $\times 10^{-4}$	$\tau_0 H$ $\times 10^{-4}$	$\tau_0 H / \tau_0 G$
NTTS 155913-2233	14.1	17.6	2.5	2.9	1.3
NTTS 160814-1857	133.8	0.6	7.5	16	2.3
NTTS 160905-1859	95.8	20.7	1.6	2.8	1.8
NTTS 162814-2427	0.6	3.0	7.4	6.1	0.8
NTTS 162819-2423S	46.0	0.3	9.3	31	3.3

Table 18. Ratio of the amplitude of the single-periodic variations over the double-periodic ones for the polarization.

Star	Ratio of the amplitude in $1\lambda$ over the amplitude in $2\lambda$				$e$	Period (d)
	$Q$	$U$	$P$	$\theta$		
LkCa 3	1.62	0.32	2.98	0.71	0.20	12.9
V826 Tau	3.31	0.49	0.63	0.75	0.0	3.9
GW Ori	0.50	1.52	0.93	0.67	0.04	242
Par 1540	0.57	0.45	0.44	0.50	0.12	33.7
Par 2494	0.56	0.68	0.69	0.56	0.26	19.5
W 134	0.60	0.60	0.68	0.29	0	6.4
NTTS 155913-2233	0.68	1.86	1.02	0.78	0.02	2.4
NTTS 160814-1857	1.26	0.13	1.80	0.72	0.26	145
NTTS 160905-1859	2.43	0.49	0.49	2.29	0.17	10.4
..... set1	1.46	1.05	1.03	1.43	0.17	10.4
..... set2	1.98	0.58	0.58	1.95	0.17	10.4
..... set3	0.91	0.59	0.59	0.91	0.17	10.4
..... set4	0.79	1.49	1.49	0.82	0.17	10.4
NTTS 162814-2427	0.52	8.11	1.74	2.73	0.48	36
NTTS 162819-2423S	0.79	0.36	0.62	0.31	0.41	89
AK Sco <sup>1</sup>	7.34	1.14	1.09	4.15	0.47	13.6
EK Cep <sup>1</sup>	0.75	1.55	0.61	4.07	0.11	4.4

Note. — The orbital eccentricities and period given are approximate values only.

<sup>1</sup>Data for AK Sco and EK Cep will be presented in future papers.